Counting nodal domains on surfaces of revolution

2008 J. Phys. A: Math. Theor. 41 205102

(http://iopscience.iop.org/1751-8121/41/20/205102)

IOP PUBLISHING JOURNAL OF PHYSICS A: MATHEMATICAL AND THEORETICAL

J. Phys. A: Math. Theor. **41** (2008) 205102 (26pp) doi:10.1088/1751-8113/41/20/205102

Counting nodal domains on surfaces of revolution

Panos D Karageorge[1,2] **and Uzy Smilansky**[1,3]

[1] School of Mathematics, University of Bristol, Bristol BS8 1TW, UK
[2] Department of Physics, University of Crete, Heraklion 71003, Greece
[3] Department of Physics of Complex Systems, The Weizmann Institute of Science, Rehovot 76100, Israel

Received 31 January 2008, in final form 20 March 2008
Published 23 April 2008
Online at stacks.iop.org/JPhysA/41/205102

Abstract

We consider eigenfunctions of the Laplace–Beltrami operator on special surfaces of revolution. For this separable system, the nodal domains of the (real) eigenfunctions form a checkerboard pattern, and their number ν_n is proportional to the product of the angular and the 'surface' quantum numbers. Arranging the wavefunctions by increasing values of the Laplace–Beltrami spectrum, we obtain the nodal sequence, whose statistical properties we study. In particular, we investigate the distribution of the normalized counts $\frac{\nu_n}{n}$ for sequences of eigenfunctions with $K \leqslant n \leqslant K + \Delta K$, where $K, \Delta K \in \mathbb{N}$. We show that the distribution approaches a limit as $K, \Delta K \to \infty$ (the classical limit), and study the leading corrections in the semi-classical limit. With this information, we derive the central result of this work: the nodal sequence of a mirror-symmetric surface is sufficient to uniquely determine its shape (modulo scaling).

PACS numbers: 02.30.Zz, 03.65.Ge, 03.65.Sq

(Some figures in this article are in colour only in the electronic version)

1. Introduction

Nodal domains of a real, continuous function are the maximally connected domains where the function does not change its sign. The nodal domains of eigenfunctions of the Laplacian on compact domains have been studied since Chladni first observed the nodal structure of vibration modes of thin plates (eigenfunctions of the bi-harmonic operator), in the early years of the 19th century. In this paper we are not interested in the geometric properties of nodal domains of Laplacian eigenfunctions, but rather in their count.

Following Courant, we order the eigenfunctions so that the corresponding eigenvalues form a non-decreasing sequence. Denoting by ν_n the number of nodal domains of the nth eigenfunction, we form the normalized nodal sequence $\xi_n := \frac{\nu_n}{n}$, $n \in \mathbb{N}$. Courant's theorem [1] guarantees that $\xi_n \leqslant 1$, and we would like to study the distribution of the values of ξ_n

in the unit interval (0, 1]. In previous papers [2, 3] the distribution of ξ_n for various planar domains and 2-manifolds were studied, and it was concluded that the features of the distribution depend crucially on the type of classical dynamics it supports. If the classical dynamics on the manifold (geodesics) are integrable (and quantum mechanically separable—for such systems, actually, quantum separability is equivalent to classical separability [4]), the limit distribution exists, and displays certain features which are common to all such systems. On the other hand, if the classical dynamics is chaotic, the distribution of the normalized nodal sequence is well reproduced by using a random wave model for the eigenfunctions [5]. Bogomolny and Schmit computed the mean and the distribution by using ideas from percolation theory [6]. Investigations on nodal domain statistics for chaotic maps with connections to percolation, involving the theory of stochastic Loewner evolution, have been made by Keating, Marklof and Williams [7].

The first work with implications on the geometric content of the nodal sequence was of Smilansky and Sankaranarayanan [3], where it was shown that the aspect ratio of a rectangular domain on the plane (with Dirichlet boundary conditions) can be determined by counting its nodal domains. In [8] the nodal sequence for eigenfunctions of the Laplace–Beltrami operator for 'simple' surfaces of revolution was discussed. A trace formula for the nodal count was derived, and was shown to depend explicitly both on some mean geometric properties of the surface, as well as the lengths of its geodesics. In spite of the formal similarity between the *spectral* and the *nodal* trace formulae, the geometrical information is included in different ways. Further studies [9–11] have shown that isospectral domains have different nodal sequences, thus supporting the conjecture that the geometrical information is stored in the nodal and spectral sequences in different ways. In the present work we go one step further and inquire whether *one can deduce the shape* (up to scaling) *of a domain given the distribution of the normalized number of nodal domains,* or, paraphrasing the classical spectral inversion question posed by Kac [12], *can one count the shape of a drum?* It must be stressed that the only use of the spectral information is lexicographical—it is ordered as a non-decreasing sequence. Otherwise, there is no reference to the actual values of the eigenvalues.

In this paper we shall confine ourselves to the integrable (and separable) case, particularly to a special class of surfaces of revolution. We present new results which pertain to the distribution $P(\xi, I_K)$ of the normalized nodal counts of eigenfunctions with indices n in the interval $I_K = [K, K + \Delta K]$. In [2] it was shown that there exists a limit distribution $P(\xi)$ when the size of the index interval I_K becomes infinite (corresponding to the semi-classical limit, $K \to \infty$). We provide the leading order term of the difference between $P(\xi, I_K)$ and the limit distribution $P(\xi)$:

$$P(\xi, I_K) = P(\xi) + \frac{1}{\sqrt{K}} P_1(\xi) + O\left(\frac{1}{K}\right). \tag{1}$$

We show that the knowledge of the function $P(\xi)$ and $P_1(\xi)$ suffices for nodal domain inversion, provided that the surface is mirror symmetric. In other words, given the normalized nodal sequence, we can deduce uniquely the profile function of the surface of revolution (provided it is smooth and symmetric). Numerical simulations were carried out for ellipsoids of revolution, which illustrate our theoretical findings.

In what follows we shall use the classical notation of asymptotic analysis; the standard 'O, o' order notation, the symbol '$\sim$' standing for an asymptotic relation, the symbol '$\asymp$' denoting the same order of magnitude and the symbol '$\gg$' denoting greater order of magnitude.

2. Surfaces of revolution

We consider surfaces of revolution $\mathcal{M}$ in $\mathbb{R}^3$, which are generated by the complete rotation of the line $y = f(x), x \in I := [-1, 1]$, about the x axis. We confine our attention to a special subset of functions which satisfy the following requirements:

(i) f^2 is analytic in I, and vanishes at ± 1, where $f(x) \sim a_\pm(1 \mp x)^{1/2}$, with $a_\pm > 0$. This requirement guarantees that $\mathcal{M}$ is compact, has no boundary and is smooth even at the points where it is intersected by the axis of rotation.

(ii) The second derivative of f is strictly negative, so that $f(x)$ has a single maximum at some $x = x_{\max}$, where it reaches the value $f_{\max}$. This requirement guarantees the convexity of $\mathcal{M}$.

Surfaces which satisfy the above requirements will be referred to as *simple surfaces of revolution*, and are convex, mild deformations of ellipsoids of revolution. The induced Riemannian metric on $\mathcal{M}$ is

$$\mathrm{d}s^2 = (1 + f'(x)^2)\,\mathrm{d}x^2 + f(x)^2\,\mathrm{d}\theta^2, \tag{2}$$

where the prime denotes differentiation with respect to x, and $\theta \in [0, 2\pi)$ is the azimuthal angle.

In the proceeding subsections we shall review the properties of geodesics (classical mechanics) and the spectrum of the Laplace–Beltrami operator (quantum mechanics) on $\mathcal{M}$.

2.1. The geodesics

The geodesics on $\mathcal{M}$ are the classical trajectories of free motion. They can be derived from the Euler–Lagrange variation principle with the Lagrangian

$$L = \tfrac{1}{2}((1 + f'(x)^2)\,\dot{x}^2 + f(x)^2\dot{\theta}^2), \tag{3}$$

where a dot above denotes time derivative. The angular momentum along the axis of rotation $f(x)^2\dot{\theta}$ is conserved, and we shall denote its value by m. The momentum conjugate to x is $p_x = (1 + f'(x)^2)\dot{x}$, and the conserved energy is

$$E = (1 + f'(x)^2)\,\dot{x}^2 + \frac{m^2}{f(x)^2}. \tag{4}$$

It is convenient to introduce the action variable n,

$$n(E, m) := \frac{1}{2\pi}\oint p_x\,\mathrm{d}x = \frac{1}{\pi}\int_{x_-}^{x_+}\sqrt{Ef(x)^2 - m^2}\,\frac{\sqrt{1 + f'(x)^2}}{f(x)}\,\mathrm{d}x. \tag{5}$$

Here, $x_\pm$ are the classical turning points, where $Ef(x)^2 - m^2 = 0$, with $x_- \leqslant x_{\max} \leqslant x_+$, which correspond to two meridians $\gamma_\pm$ (projections of caustics onto $\mathcal{M}$) between which all geodesics with $m \neq 0$ wind around $\mathcal{M}$. Real classical trajectories exist only if $E > (m/f_{\max})^2$. The convexity of $\mathcal{M}$ guarantees that the action variables (n, m) along with their conjugate angle variables constitute a global coordinate system on phase space [13].

The classical Hamiltonian $H(n, m)$ in the action–angle representation is obtained by inverting (5) to express the energy in terms of n and m. $H(n, m)$ is a homogeneous function of order 2, i.e. $H(\lambda n, \lambda m) = \lambda^2 H(n, m),\ \lambda > 0$ [14]. It suffices, therefore, to study the function $n(m) := n(1, m)$, which defines a smooth line Γ in the (n, m)-plane (the projection of the unit energy shell on the action plane). The function $n(m)$ is one of the main building blocks of the semi-classical theory which will be used throughout this work. We shall list some of its properties which will be used in the following:

(i) The reflection symmetry, $n(-m) = n(m)$, follows from definition (5). Thus, we restrict our attention to $m \geqslant 0$ when referring to Γ.

(ii) $n(|m|)$ is defined in the interval $I_\mu = (0, m_{\max}]$, where $m_{\max} = f_{\max}$. In this interval, $n(m)$ is analytic and decreases monotonically since

$$\frac{\mathrm{d}n(m)}{\mathrm{d}m} = -\frac{m}{\pi}\int_{x_-}^{x_+} \frac{1}{\sqrt{f(x)^2 - m^2}} \frac{\sqrt{1 + f'(x)^2}}{f(x)}\,\mathrm{d}x \leqslant 0. \tag{6}$$

(iii) $n(m)$ assumes its maximum value at $m = 0$,

$$n(0) = \frac{1}{\pi}\int_{-1}^{1} \sqrt{1 + f'(x)^2}\,\mathrm{d}x = \frac{\mathcal{L}}{\pi}, \tag{7}$$

where $\mathcal{L}$ is the length of the rotating line. We show in appendix A that $n(m)$ is not analytic at $m = 0$, and in that vicinity

$$n(m) \sim \frac{\mathcal{L}}{\pi} - |m|. \tag{8}$$

At the other endpoint, $n(m)$ vanishes,

$$n(m) \sim \sqrt{\frac{2}{\omega}}(m_{\max} - m), \qquad \omega = |2m_{\max} f''(x_{\max})|. \tag{9}$$

(iv) The phase space volume is

$$\frac{1}{(2\pi)^2}\int_{\mathbb{R}^2_+} \Theta(E - H(n, m))\,\mathrm{d}v = 2E\int_0^{m_{\max}} n(m)\,\mathrm{d}m = 2\mathcal{A}E. \tag{10}$$

$\mathcal{A}$ is the area enclosed between the line Γ and the n and m axes. It is related to the area of $\mathcal{M}$ by $||\mathcal{M}|| = 8\pi\mathcal{A}$.

(v) The computation of the higher derivatives of $n(m)$ cannot proceed simply by taking the derivatives of (6)—the resulting integrals diverge. To overcome this difficulty the integral defining $n(m)$ needs regularization [15]. This is done in appendix A.

(vi) Some authors (e.g., [14]) prefer to use the Clairaut integral $\mathcal{I}$ instead of the angular momentum. They are related by

$$\mathcal{I} = \frac{m}{\sqrt{2E}}. \tag{11}$$

The *twist condition* is introduced in [14] to distinguish the class of simple surfaces of revolution, for which the dynamics are particularly simple. In the present notation, the twist condition is expressed by the requirement

$$\frac{\partial^2 n(E, m)}{\partial m^2} \neq 0, \qquad 0 < |m| \leqslant m_{\max}, \tag{12}$$

i.e. $n(m)$ is either convex or concave on $(0, m_{\max})$.

Throughout this paper we shall use the ellipsoid of revolution to illustrate our findings graphically. The ellipsoids are generated by $f(x)^2 = \varepsilon^2(1 - x^2)$, with $\varepsilon > 0$ being the eccentricity of the generating semi-ellipse.

For the ellipsoid, the action variable $n(m)$ reduces to

$$n(m) = \frac{2x_\pm^2}{\pi}\int_0^1 \frac{\sqrt{1 - t^2}}{1 - x_\pm^2 t^2}\sqrt{1 - (1 - \varepsilon^2)x_\pm^2 t^2}\,\mathrm{d}t, \tag{13}$$

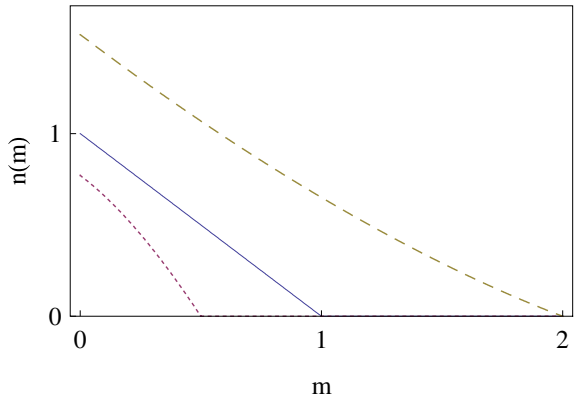

Figure 1. The curves Γ for ellipsoids of revolution with eccentricities $\varepsilon = 0.5$ (prolate), $\varepsilon = 1$ (a sphere) and $\varepsilon = 2$ (oblate) are shown as dashed line, solid line and sparsely dashed line, respectively.

where $x_\pm = \pm\sqrt{1 - m^2/\varepsilon^2}$ are the classical turning points. This integral can be evaluated in terms of elliptic functions giving

$$n(m) = \frac{2}{\pi}\frac{1}{\varepsilon\sqrt{b}}\left[b\mathrm{E}\left(1-\frac{\varepsilon^2}{b}\right) - (1-\varepsilon^2)m^2\,\mathrm{K}\left(1-\frac{\varepsilon^2}{b}\right) - \varepsilon^4\Pi\left(1-\frac{\varepsilon^2}{m^2}, 1-\frac{\varepsilon^2}{b}\right)\right], \tag{14}$$

where $b = \varepsilon^4 + (1-\varepsilon^2)m^2$, and

$$\mathrm{K}(k) := \int_0^{\pi/2} (1 - k\sin^2\theta)^{-1/2}\,\mathrm{d}\theta,$$

$$\mathrm{E}(k) := \int_0^{\pi/2} (1 - k\sin^2\theta)^{1/2}\,\mathrm{d}\theta,$$

$$\Pi(k,l) := \int_0^{\pi/2} (1 - k\sin^2\theta)^{-1}(1 - l\sin^2\theta)^{-1/2}\,\mathrm{d}\theta$$

are the complete elliptic integrals of the first, second and third kinds, respectively.

Figure 1 shows the functions $\Gamma := n(m)$ for a few ellipsoids of revolution

2.2. The Laplace–Beltrami operator

The Laplace–Beltrami operator on $\mathcal{M}$ reads

$$\Delta = -\frac{1}{f(x)\sigma(x)}\frac{\partial}{\partial x}\frac{f(x)}{\sigma(x)}\frac{\partial}{\partial x} - \frac{1}{f(x)^2}\frac{\partial^2}{\partial\theta^2}, \tag{15}$$

where $\sigma(x) := \sqrt{1 + f'(x)^2}$. The domain of Δ are $\Psi \in W_2^2(I \times \mathbb{S}^1)$ (the class of L^2 wavefunctions all of whose partial derivatives, up to second, are also L^2), required to be 2π-periodic in θ. Under these conditions, the operator is self-adjoint, and its spectrum is discrete and non-negative. Δ is separable, and the eigenfunctions can be written in the product form $\Psi(x,\theta) = \exp(\mathrm{i}m\theta)\psi_m(x)$, where $m \in \mathbb{Z}$. It is convenient to introduce a new variable t, through

$$\mathrm{d}t = \frac{\sigma(x)}{f(x)}\,\mathrm{d}x, \tag{16}$$

which maps the interval $[-1, 1]$ to $\mathbb{R} \cup \{\infty\}$. For any m and eigenvalue $E_{n,m}$, the spectral equation for (15) reduces to the Sturm–Liouville ODE

$$\left[-\frac{\mathrm{d}^2}{\mathrm{d}t^2} + (m^2 - E_{n,m} f(x(t))^2)\right] \psi_{n,m}(t) = 0. \tag{17}$$

The spectrum of the Laplace–Beltrami operator is doubly degenerate for all $m \neq 0$, with $E_{n,-m} = E_{n,m}$. The semi-classical spectrum is constructed by using the Einstein–Brillouin–Keller approximation [14],

$$E^{\mathrm{scl}}_{n,m} = H\left(n + \tfrac{1}{2}, m\right), \qquad n \in \mathbb{N}_0, \qquad m \in \mathbb{Z}, \tag{18}$$

where $H(n, m)$ is the classical Hamiltonian defined in terms of the action variables. The semi-classical approximation for the spectral sequence with $m = 0$ assumes a very simple form. Since

$$n + \frac{1}{2} = \frac{\sqrt{E}}{\pi} \int_{-1}^{1} \sqrt{1 + f'(x)^2}\, \mathrm{d}x = \frac{\sqrt{E}}{\pi} \mathcal{L}, \tag{19}$$

the semi-classical quantization condition reads

$$E^{\mathrm{scl}}_{n,0} = \left[\frac{\pi\left(n + \frac{1}{2}\right)}{\mathcal{L}}\right]^2, \qquad n \in \mathbb{N}_0. \tag{20}$$

Because of the degeneracy of the spectrum, we have to choose a particular representation of the wavefunctions. We do this by associating $\cos(m\theta)$ with $m \geqslant 0$ and $\sin(m\theta)$ for $m < 0$, i.e.,

$$\Psi_{n,m}(x, \theta) = \psi_{n,m}(x) \begin{cases} \sin(m\theta) & \text{if} \quad m < 0 \\ \cos(m\theta) & \text{if} \quad m \geqslant 0. \end{cases} \tag{21}$$

The nodal pattern of Ψ is that of a checkerboard, typical for separable systems (as a matter of fact, the nodal pattern remains a checkerboard for any linear combination of the basis functions. It is only rotated around the symmetry axis of the surface). For $m = 0$, the number of nodal domains is $\nu_{n,0} = n + 1$, and for all other m, $\nu_{n,m} = 2(n+1)|m|$. In summary,

$$\nu_{n,m} = (n + 1)(2|m| + \delta_{m,0}). \tag{22}$$

To end this section we illustrate its content by an application to the simplest surface—the sphere, considered here as a surface of revolution with $f(x)^2 = 1 - x^2$.

For the sphere, the action variable (5) takes the simple form

$$n(E, m) = \frac{2\sqrt{E}}{\pi} \int_0^{\sqrt{1-m^2/E}} \frac{\sqrt{1 - m^2/E - x^2}}{1 - x^2}\, \mathrm{d}x = \sqrt{E} - |m|. \tag{23}$$

Thus, $H(n, m) = (n + |m|)^2$, and the EBK quantization for the spectrum is $E_{n,m} = \left(l + \frac{1}{2}\right)^2 \sim l(l + 1)$, where $l := n + |m|$. The $(2l + 1)$-fold degeneracy follows immediately by counting the number of integer pairs (n, m) which satisfy $l = n + |m|$.

Turning to the quantum description, the variable t defined in (16) can be explicitly computed, $x = \tanh t$. Writing $E = l(l + 1)$, $l \in \mathbb{N}_0$, transforms (17) to

$$\left[-\frac{\mathrm{d}^2}{\mathrm{d}t^2} + \left(m^2 - \frac{l(l + 1)}{\cosh^2 t}\right)\right] \psi_{l,m}(t) = 0, \tag{24}$$

which is equivalent to the Legendre equation. Finally, the number of nodal domains of spherical harmonics is known, and coincides with (22) when the identification $l = n + |m|$ is made.

3. Counting nodal domains

We shall start this section by reviewing some of the general definitions and results obtained in [2], where the limit distribution of the normalized nodal counts was first studied. We shall then derive the next to leading term, and show that it provides further information on the geometry of $\mathcal{M}$.

The nodal structure of the wavefunctions was reviewed in the preceding section, and an explicit expression for the dependence of the number of nodal domains $\nu_{n,m}$ on the quantum numbers (n, m) is given in (22).

The object which is investigated in this work is the *nodal sequence* which is defined as follows: arrange the spectrum as a non-decreasing sequence. This amounts to assigning to each pair of quantum numbers (n, m) a counting index $\mathcal{N}(n, m)$, which gives the number of eigenvalues of the Laplace–Beltrami operator (counted with multiplicity) which are *strictly* smaller than the eigenvalue $E_{n,m}$, i.e. $\mathcal{N}(n, m) := \#\{E \in \mathrm{Spec}(\Delta) : E < E_{n,m}\}$. Obviously $\mathcal{N}(n, m) = N(E_{n,m})$, where $N(E)$ is the spectral counting function.

To account for the spectral degeneracy, we modify the above definition for $|m| \neq 0$, so that $\mathcal{N}(n, |m|) = \mathcal{N}(n, -|m|)+1$. The nodal sequence is the sequence of nodal counts ordered by $\mathcal{N}$: $\{\nu_{\mathcal{N}}\}_{\mathcal{N}=1}^{\infty}$. By this convention, the systematic degeneracy of the spectrum is taken care of. In general, however, accidental degeneracies cannot be excluded. The ordering ambiguity may appear, e.g., when the degeneracy class involves states with different (non-negative) m values, such as, e.g., for the sphere. In this case, a possible way to remove this problem is to consider the sphere as a limiting case of an ellipsoid with (a positive) eccentricity approaching one (here we use the particular convention for the eccentricity, for which it equals unity for the sphere, and not zero). The m degeneracy is removed for any ellipsoid, and the order of the eigenvalues is monotonic in $|m|$ for arbitrary small eccentricity. Similar constructions can be used for other accidental degeneracies.

Courant's theorem [1] ensures that, for any ordering of the eigenfunctions in the degeneracy classes

$$\nu_{\mathcal{N}(n,m)} \leqslant \mathcal{N}(n, m). \tag{25}$$

It is natural, therefore, to define the *normalized nodal sequence*

$$\xi_{\mathcal{N}} := \frac{\nu_{\mathcal{N}}}{\mathcal{N}}, \qquad 0 < \xi_{\mathcal{N}} \leqslant 1. \tag{26}$$

We study the distribution of the values of the normalized nodal sequence for a finite index set, $\mathcal{N} \in \{K, \ldots, K + \Delta K\}$,

$$P(\xi, I_K) := \frac{1}{\Delta K} \sum_{(n,m)\in\mathbb{N}_0\times\mathbb{Z}} \chi_{I_K}(\mathcal{N}(n, m))\delta(\xi - \xi_{\mathcal{N}(n,m)}), \tag{27}$$

and χ_{I_K} the characteristic function of the interval I_K,

$$\chi_{I_K}(x) = \begin{cases} 1 & \text{if} \quad K \leqslant x \leqslant K + \Delta K \\ 0 & \text{otherwise.} \end{cases} \tag{28}$$

Since $P(\xi, I_K)$ is not a function but a distribution over the interval $(0, 1)$, one must take care in its manipulations. Most of the limits and estimates are considered in the weak sense (e.g. [16]). In some sections though, related distributions are viewed as functions (or to be more precise, the functions whose values these distributions take on some subinterval of $(0, 1)$). In other cases they will be manipulated as functions after an appropriate regularization.

In [2], it was assumed for convenience that I_K grows linearly in K, $\Delta K = gK$, g being a positive constant (such that $gK \in \mathbb{N}$). The existence of the limiting distribution $P(\xi)$ of

$P(\xi, I_K)$ in the $K \to \infty$ limit (the classical limit) was proved, and its universal features were presented. The existence can be proven by showing

$$\frac{1}{\Delta K} \sum_{j \in I_K} \varphi(\xi_j) \longrightarrow \int_0^1 P(\xi)\varphi(\xi)\, \mathrm{d}\xi \tag{29}$$

uniformly in g, for any smooth and compactly supported test function φ on $(0, 1)$. Here, we shall repeat the derivation in more detail, and also compute the difference between $P(\xi, I_K)$ and $P(\xi)$ to leading order in $\frac{1}{\sqrt{K}}$ (again, for the linear case $\Delta K = gK$—the superlinear case $\Delta K \gg K$, follows trivially).

We rewrite (27) as a sum of an isotropic component, to which only isotropic states (with $m = 0$) contribute, and an anisotropic component (with $m \neq 0$),

$$\begin{aligned} P(\xi, I_K) &= P_{m=0}(\xi, I_K) + P_{m\neq 0}(\xi, I_K), \\ P_{m=0}(\xi, I_K) &= \frac{1}{gK} \sum_n \chi_{I_K}(\mathcal{N}(n, 0))\, \delta\left(\xi - \frac{n+1}{\mathcal{N}(n, 0)}\right), \\ P_{m\neq 0}(\xi, I_K) &= \frac{1}{gK} \sum_{n,m\neq 0} \chi_{I_K}(\mathcal{N}(n, m))\, \delta\left(\xi - \frac{2(n+1)|m|}{\mathcal{N}(n, m)}\right). \end{aligned} \tag{30}$$

Since we are interested in the semi-classical limit, we are allowed to make the following approximate steps, which incur errors of order higher than $O\left(\frac{1}{\sqrt{K}}\right)$.

(i) The spectrum is approximated by $E_{n,m} \sim E^{\mathrm{scl}}_{n,m} = H\left(n + \frac{1}{2}, m\right)$, as $m^2 + n^2 \to \infty$, which introduces a relative error bounded by $O\left(\frac{1}{E_{n,m}}\right)$ [17]. In particular, as was shown in (20), $E^{\mathrm{scl}}_{n,0} = \left[\frac{\pi(n+\frac{1}{2})}{\mathcal{L}}\right]^2$.

(ii) To the same order, $\mathcal{N}(n, m)$ can be replaced by the first term in the Weyl series [14],

$$\mathcal{N}(n, m) = 2\mathcal{A}H\left(n + \frac{1}{2}, m\right)\left(1 + O\left(\frac{1}{E^{\frac{3}{4}}_{n,m}}\right)\right), \tag{31}$$

where $\mathcal{A}$ is defined in (10).

Introducing these approximations in (30), we find that $P_{m=0}(\xi, I_K)$ is $O\left(\frac{1}{K}\right)$ (in the weak sense) and therefore we defer its computation to a later stage. The sums over (n, m) in (30) are computed using the Poisson summation formula, decomposing $P_{m\neq 0}(\xi, I_K)$ in a smooth and an oscillatory part,

$$P_{m\neq 0}(\xi, I_K) = \bar{P}(\xi, I_K) + Q(\xi, I_K) := \bar{P}(\xi, I_K) + \sum_{(N,M)\in\mathbb{Z}^2\setminus\{0\}} Q_{N,M}(\xi, I_K), \tag{32}$$

where the Fourier coefficients are

$$\begin{aligned} Q_{N,M}(\xi, I_K) \sim \frac{2}{gK} \int_{\frac{1}{2}}^{\infty} \mathrm{d}m \int_{-\frac{1}{2}}^{\infty} \mathrm{e}^{2\pi \mathrm{i}(Mm+Nn)} \chi_{I_K}\left(2\mathcal{A}H\left(n + \frac{1}{2}, m\right)\right) \\ \times \delta\left(\xi - \frac{2(n+1)m}{2\mathcal{A}H\left(n + \frac{1}{2}, m\right)}\right) \mathrm{d}n, \end{aligned} \tag{33}$$

and obviously $\bar{P}(\xi, I_K) = Q_{0,0}(\xi, I_K)$.

The leading term in the above sum is the smooth term $\bar{P}(\xi, I_K)$ which we calculate first. The oscillatory terms are of lower order in $\frac{1}{\sqrt{K}}$ and will be computed in a separate subsection.

Proceeding with the smooth part, we shift the integration variable $n \mapsto n + \frac{1}{2}$ and write the result as

$$\bar{P}(\xi, I_K) \sim \frac{2}{gK} \int_{\frac{1}{2}}^{\infty} \mathrm{d}m \int_0^{\infty} \chi_{I_K}(2\mathcal{A}H(n,m))\delta\left(\xi - \frac{\left(n+\frac{1}{2}\right)m}{\mathcal{A}H(n,m)}\right)\mathrm{d}n. \quad (34)$$

We change the integration variables $(n, m) \mapsto (\mathcal{E}, s)$, where $\mathcal{E} = H(n, m)$, and s is defined through the relations

$$\mathrm{d}\mathcal{E} = \omega_n \mathrm{d}n + \omega_m \mathrm{d}m, \qquad \omega_n = \frac{\partial H(n,m)}{\partial n}, \qquad \omega_m = \frac{\partial H(n,m)}{\partial m},$$
$$\mathrm{d}s = \frac{-\omega_m \mathrm{d}n + \omega_n \mathrm{d}m}{\omega_n^2 + \omega_m^2}. \quad (35)$$

Note that with this definition the Jacobian is unity, and $\mathrm{d}n\mathrm{d}m = \mathrm{d}\mathcal{E}\mathrm{d}s$. Thus, (34) is reduced to

$$\bar{P}(\xi, I_K) \sim \frac{2}{gK} \int_{\frac{K}{2\mathcal{A}}}^{\frac{K(1+g)}{2\mathcal{A}}} \mathrm{d}\mathcal{E} \int_{\Gamma} \Theta\left(m(s) - \frac{1}{2\sqrt{\mathcal{E}}}\right)\delta\left(\xi - \frac{n(s)m(s)}{\mathcal{A}} - \frac{m(s)}{2\sqrt{\mathcal{E}}\mathcal{A}}\right)\mathrm{d}s, \quad (36)$$

where $\Theta(x)$ is the Heaviside step function. The pair of functions $\{n(s), m(s)\}$ constitute a parametric representation of the line Γ, along which $H(n(s), m(s)) = 1$. This allows the scaling by $\sqrt{\mathcal{E}}$ which appears in (36).

The above expression can be further reduced by the following observation. On the line Γ we have $\omega_n \mathrm{d}n + \omega_m \mathrm{d}m = 0$, which induces a symplectic structure (where n and m play the roles of canonically conjugate variables and s is the 'time'):

$$\frac{\mathrm{d}m(s)}{\mathrm{d}s} = \omega_n, \qquad \frac{\mathrm{d}n(s)}{\mathrm{d}s} = -\omega_m. \quad (37)$$

Another important identity follows from the fact that $H(n, m)$ is homogeneous of order 2 in (n, m). We can write $n = F(H, m)$, and $\frac{n}{\sqrt{H}} = F\left(1, \frac{m}{\sqrt{H}}\right)$, from which we deduce that on the line $\{H(n, m) = 1\}$,

$$\frac{\mathrm{d}m(s)}{\mathrm{d}s} = \omega_n = \frac{2}{n(m) - mn'(m)}, \quad (38)$$

where $n'(m) := \frac{\mathrm{d}n(m)}{\mathrm{d}m}$. Thus, (36) takes the form

$$\bar{P}(\xi, I_K) \sim \frac{1}{gK} \int_{\frac{K}{2\mathcal{A}}}^{\frac{K(1+g)}{2\mathcal{A}}} \mathrm{d}\mathcal{E} \int_{\frac{1}{2\sqrt{\mathcal{E}}}}^{m_{\max}} |n(m) - mn'(m)|\delta\left(\xi - \frac{n(m)m}{\mathcal{A}} - \frac{m}{2\sqrt{\mathcal{E}}\mathcal{A}}\right)\mathrm{d}m. \quad (39)$$

A similar transformation can also be applied in the computation of the oscillatory integrals $Q_{N,M}(\xi, I_K)$.

3.1. The limit distribution

The limit distribution is the leading term in the expansion of the integral (36) in powers of $\frac{1}{\sqrt{K}}$. Taking the limit $K \to \infty$, the $\mathcal{E}$-integral can be directly performed, resulting with

$$P(\xi) = \frac{1}{\mathcal{A}} \int_{\Gamma} \delta\left(\xi - \frac{m(s)n(s)}{\mathcal{A}}\right)\mathrm{d}s. \quad (40)$$

This expression allows a simple geometrical interpretation: the product $n(s)m(s)$ is the area of the rectangle whose vertices are the points $(m(s), n(s))$ on Γ, its projections $(m(s), 0)$ and $(0, n(s))$ on the two axes and the origin (see figure 2). $P(\xi)$ is the probability distribution of the areas of these rectangles (scaled by $\mathcal{A}$, and therefore smaller than 1). The areas of

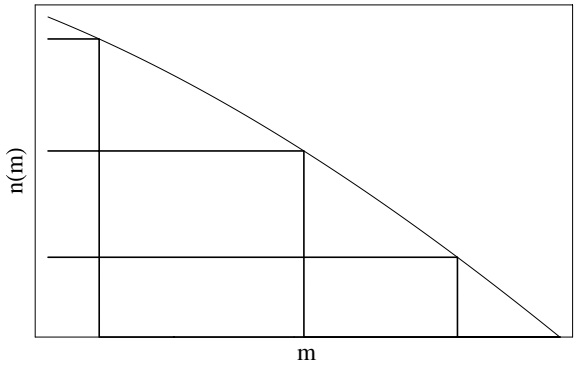

Figure 2. The geometric interpretation of $P(\xi)$ (computed for an ellipsoid of revolution with eccentricity $\varepsilon = 0.5$).

rectangles which are based on points which are either near the m or the n axes approach 0. Since Γ is either convex or concave, there exists a unique point where ξ reaches the maximal value of scaled areas, $\xi_{\max}$. Thus, $P(\xi) \equiv 0$ for $\xi \geqslant \xi_{\max}$.

Changing integration variables using (38), we get

$$P(\xi) = \frac{1}{2\mathcal{A}} \int_0^{m_{\max}} \delta\left(\xi - \frac{mn(m)}{\mathcal{A}}\right) |n(m) - mn'(m)| \mathrm{d}m. \tag{41}$$

Integrating (41), we get

$$P(\xi) = \begin{cases} 0 & \xi \geqslant \xi_{\max}, \\ \dfrac{1}{2} \sum \left| \dfrac{n(m) - mn'(m)}{n(m) + mn'(m)} \right|_{\xi = \frac{mn(m)}{\mathcal{A}}} & \xi < \xi_{\max}. \end{cases} \tag{42}$$

The sum is over the real values of $m > 0$ which satisfy $\xi = \frac{mn(m)}{\mathcal{A}}$. In the vicinity of $\xi_{\max}$, typically two solutions coalesce, leading to a square-root singularity of $P(\xi)$ at that point. The vanishing of $P(\xi)$ in the interval $[\xi_{\max}, 1]$, and the square-root singularity at $\xi_{\max}$ are the universal features which characterize the nodal domain distributions for separable systems (in 2D) in general, and simple surfaces of revolution, in particular. Using (41), it is easy to check normalization, $\int_0^1 P(\xi)\, \mathrm{d}\xi = 1$.

Form (42) for the ξ distribution can be further simplified since for simple surfaces of revolution the twist condition (12) is satisfied, and there are only two values of m which solve $\xi = \frac{mn(m)}{\mathcal{A}}$. Denote them by $m_-(\xi)$ and $m_+(\xi)$ ($m_-(\xi) \leqslant m_+(\xi)$). They coalesce at $\xi = \xi_{\max}$. The value of m where the sole maximum of $mn(m)$ occurs is denoted by $m_0 = m_\pm(\xi_{\max})$. The two functions $m_+(\xi)$ and $m_-(\xi)$, together, provide a parametric representation of the curve Γ, since $n_\pm(\xi) = \frac{\mathcal{A}\xi}{m_\pm(\xi)}$, where $0 < \xi < \xi_{\max}$. This parametrization will be used often in the subsequent discussion.

To leading order, $m_\pm(\xi) \sim m_0(1 \pm \sqrt{|\zeta|})$, where $\zeta = \frac{\xi - \xi_{\max}}{\xi_{\max}}$, and so from (42) we deduce that, in the left neighbourhood of $\xi_{\max}$

$$P(\xi) \sim \frac{1}{\sqrt{1 - \xi/\xi_{\max}}}. \tag{43}$$

One can re-arrange (42) to obtain another expression for the limiting distribution. For $\xi < \xi_{\max}$,

$$P(\xi) = \xi \frac{\mathrm{d}}{\mathrm{d}\xi} \log \frac{m_-(\xi)}{m_+(\xi)}. \tag{44}$$

This expression is quite revealing, because it can be inverted to provide the function $\frac{m_-(\xi)}{m_+(\xi)}$ based on the information derived only from the nodal sequence. We shall show below that the next to leading expression in the expansion of $P(\xi, I_K)$ provides another relation between $m_-(\xi)$ and $m_+(\xi)$. On solving the two equations, we obtain a complete parametric representation of the curve Γ (or $n(m)$). We shall also show that Γ defines uniquely the function $f(x)$, when $f(x)$ is symmetric about $x = 0$. This will prove our claim that the nodal sequence for symmetric surfaces of revolution can be inverted and provide the 'shape of the drum'!

The behaviour of $P(\xi)$ near $\xi = 0$ can be easily extracted using (44). Since $\xi \to 0$ implies either $m \to 0$ or $n(m) \to 0$ along Γ, we may use the linear approximations for $n(m)$ as given by (8) and (9), respectively. The equation $\frac{mn(m)}{\mathcal{A}} = \xi$ reduces to a quadratic equation, and its solutions define the two branches $m_-(\xi)$ and $m_+(\xi)$ as

$$\begin{aligned} m_-(\xi) &\sim \frac{\mathcal{L}}{2\pi}\left(1 - \sqrt{1 - 2\xi\frac{2\mathcal{A}\pi^2}{\mathcal{L}^2}}\right), \\ m_+(\xi) &\sim \frac{m_{\max}}{2}\left(1 + \sqrt{1 - 2\xi\frac{\mathcal{A}\sqrt{2\omega}}{m_{\max}^2}}\right). \end{aligned} \tag{45}$$

Substituting in (44), we get

$$P(\xi) \sim \frac{1}{2}\left(\frac{1}{\sqrt{1 - \frac{2\xi}{\eta_-}}} + \frac{1}{\sqrt{1 - \frac{2\xi}{\eta_+}}}\right), \tag{46}$$

where

$$\eta_- = \frac{n(0)^2}{2\mathcal{A}} = \frac{\mathcal{L}^2}{2\pi^2\mathcal{A}}, \qquad \eta_+ = \frac{|n'(m_{\max})|m_{\max}^2}{2\mathcal{A}} = \frac{m_{\max}^2}{\sqrt{2\omega}\mathcal{A}}, \qquad \eta_0 = \frac{m_{\max}^2}{2\mathcal{A}}. \tag{47}$$

Relation (46) shows that $\lim_{\xi\to 0+} P(\xi) = 1$, independently of the surface under consideration—another universal feature to be added to the aforementioned ones. Moreover, it shows that one can extract the dimensionless geometric parameters η_- and η_+ from $P(\xi)$ in the neighbourhood of $\xi = 0$. They are directly related to the properties of the line which generates $\mathcal{M}$ through its length, maximum distance from the axis of revolution and its curvature at the maximum. Note, however, that the nodal sequence is composed of integers, and in contrast to the spectral sequence it is invariant under isotropic scalings on $\mathcal{M}$. Therefore, only dimensionless quantities can be extracted from it. Here, all the lengths are expressed in units of $\sqrt{\mathcal{A}}$. (The parameter η_0 in (47) is another dimensionless parameter which we define here even though it will appear only later.)

The limit distributions for three ellipsoids of revolution are shown in figure 3. Computing $\xi_{\max}$ as a function of the eccentricity reveals that $\xi_{\max}(\varepsilon)$ is a monotonically decreasing function which varies between $\xi_{\max}(0) \approx 0.550$ and $\xi_{\max}(\infty) \approx 0.464$ as shown in figure 4. Thus, one can deduce the eccentricity from the nodal sequence just by determining the support of $P(\xi)$.

As another application of (44), and as an illustration, we derive $P(\xi)$ for the sphere. From (A.12) we get that for the sphere $n(m) = 1 - m$ which immediately gives

$$P(\xi) = \frac{1}{\sqrt{1 - 2\xi}}, \qquad 0 < \xi < \frac{1}{2}. \tag{48}$$

The same result can also be obtained directly. The spectrum consists of the values $E_{n,m} = n(n+1)$ which are independent of m ($|m| \leqslant n$) and are $(2n+1)$-fold degenerate. The eigenfunctions are the spherical harmonics, and for the sake of counting their nodal domains,

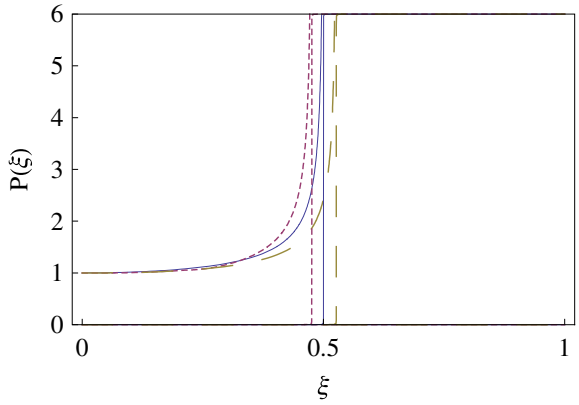

Figure 3. $P(\xi)$ for ellipsoids of revolution with eccentricities $\varepsilon = 0.5$, 1 and 2 (sparsely dashed line, solid line and dashed line, respectively).

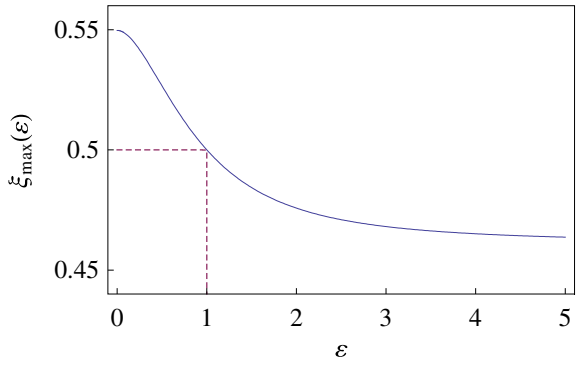

Figure 4. $\xi_{\max}$ as a monotonically decreasing function of the eccentricity ε for ellipsoids of revolution. The dashed line marks $\varepsilon = 1$, the sphere, for which $\xi_{\max} = 0.5$ as in (48).

we consider them in their separable basis. The number of zeros of $P_n^m(\cos\theta)$ is n when $m = 0$, and $n - |m| + 2$ otherwise. The number of nodal domains are, respectively, $n + 1$ and $2|m|(n - |m| + 1)$. The counting function for the $2n + 1$ degenerate states with a given n satisfies

$$n^2 \leqslant \mathcal{N}(n, m) < (n + 1)^2. \tag{49}$$

The ordering within the set is arbitrary, but in the limit of large n it is immaterial, since to leading order we can write $\mathcal{N}(n, m) = n(n + 1)\left(1 + O\left(\frac{1}{n}\right)\right)$. Hence, the contribution of the n-fold degenerate set to $P(\xi)$ is

$$\begin{aligned} P(\xi; n) &= \frac{1}{n}\sum_{m=1}^{n} \delta\left(\xi - \frac{2m(n - m + 1)}{n(n + 1)}\right) + O\left(\frac{1}{n}\right) \\ &\to \int_0^1 \delta(\xi - 2\mu(1 - \mu))\,\mathrm{d}\mu = \frac{1}{\sqrt{1 - 2\xi}}. \end{aligned} \tag{50}$$

3.2. The next to leading terms

Several terms contribute $O\left(\frac{1}{\sqrt{K}}\right)$ corrections. In the following we shall address them in detail.

3.2.1. The leading correction to $\bar{P}(\xi, I_K)$. Starting again from (39), we see that the m-integration results in a sum of two terms, coming from the two branches of solutions of $\xi = \frac{mn(m)}{\mathcal{A}} + \frac{m}{2\sqrt{\mathcal{E}}\mathcal{A}} + O\left(\frac{1}{\mathcal{E}}\right)$ which constitute the two-point support of the δ function in the integral. They differ by an amount $\delta m_\pm(\xi)$ of $O\left(\frac{1}{\sqrt{\mathcal{E}}}\right)$ from the values $m_\pm(\xi)$ which were introduced for computation (44) of the limit distribution,

$$\delta m_\pm(\xi) = -\frac{1}{2\sqrt{\mathcal{E}}}\frac{m}{mn'(m)+n(m)} + O\left(\frac{1}{\mathcal{E}}\right), \qquad \text{computed at } m = m_\pm(\xi). \tag{51}$$

As long as $(m + \delta m)_\pm$ remain inside the integration range, one can proceed with the computation towards the semi-classical asymptotic expansion

$$\bar{P}(I_K) = P + \frac{1}{\sqrt{K}}P_1 + O\left(\frac{1}{K}\right). \tag{52}$$

Of course, P is the limit distribution (42), and

$$P_1(\xi) = -\sqrt{\frac{\mathcal{A}}{2}}\frac{\sqrt{1+g}-1}{g}(p_-(\xi)+p_+(\xi)), \tag{53}$$

where $p_\pm(\xi)$ are given by

$$p_\pm(\xi) = \frac{\frac{1}{n(m)}}{1+m\frac{n'(m)}{n(m)}}\left|\frac{1-m\frac{n'(m)}{n(m)}}{1+m\frac{n'(m)}{n(m)}}\right|\left[-1+\frac{2m\left(m\frac{n'(m)}{n(m)}\right)'}{1-\left(m\frac{n'(m)}{n(m)}\right)^2}\right], \quad \text{computed at } m = m_\pm(\xi). \tag{54}$$

These expressions can be further simplified. To do so, we differentiate $m_\pm(\xi)n(m_\pm(\xi)) = \mathcal{A}\xi$ with respect to ξ and get

$$n = \frac{\mathcal{A}\xi}{m}, \qquad n' = n\left(\frac{1}{\xi\frac{\mathrm{d}m}{\mathrm{d}\xi}} - \frac{1}{m}\right), \qquad n'' = n\left(\frac{2}{m^2} - \frac{2}{\xi m\frac{\mathrm{d}m}{\mathrm{d}\xi}} - \frac{\frac{\mathrm{d}^2m}{\mathrm{d}\xi^2}}{\xi\left(\frac{\mathrm{d}m}{\mathrm{d}\xi}\right)^3}\right), \tag{55}$$

computed at $m = m_\pm(\xi)$. By substituting the above in the defining expressions for $p_\pm(\xi)$, we obtain after some straightforward calculations

$$p_\pm(\xi) = \pm\frac{1}{\mathcal{A}}\left(\frac{\mathrm{d}m_\pm}{\mathrm{d}\xi} + 2\xi\frac{\mathrm{d}^2m_\pm}{\mathrm{d}\xi^2}\right) = \pm\frac{2}{\mathcal{A}}\sqrt{\xi}\frac{\mathrm{d}}{\mathrm{d}\xi}\left(\sqrt{\xi}\frac{\mathrm{d}m_\pm}{\mathrm{d}\xi}\right). \tag{56}$$

Hence,

$$P_1(\xi) = -\sqrt{\frac{2}{\mathcal{A}}}\frac{\sqrt{1+g}-1}{g}\sqrt{\xi}\frac{\mathrm{d}}{\mathrm{d}\xi}\left(\sqrt{\xi}\frac{\mathrm{d}}{\mathrm{d}\xi}[m_+(\xi)-m_-(\xi)]\right). \tag{57}$$

This is an explicit expression which provides the leading correction in terms of the difference $m_+(\xi) - m_-(\xi)$ between the two branches of the parametric representation of Γ. Together with (44) it forms the basis for the inversion procedure which will be discussed in detail in the following section.

The conditions for the validity of the above approximation are not satisfied if ξ is in the $O\left(\frac{1}{\sqrt{K}}\right)$ neighbourhood of either 0 or $\xi_{\max}$. Near $\xi_{\max}$ (51) diverges, while near $\xi = 0$, $(m + \delta m)_\pm$ may lie outside of the integration range $\left[\frac{1}{2\sqrt{\mathcal{E}}}, m_{\max}\right]$. To get the correct

expressions for $\bar{P}(\xi, I_K)$ in the vicinity of the extreme values of ξ, we use several variations of the same trick: within the problematic domains of integration, we approximate $n(m)$ as a linear function of m. The argument of the δ functions become quadratic functions of m. The support of the δ functions can be evaluated explicitly, and the m-integrations can be performed exactly. The remaining $\mathcal{E}$-integrations turn out to be straightforward, so that explicit expressions for $\bar{P}(\xi, I_K)$ in the vicinity of $\xi = 0$ and $\xi = \xi_{\max}$ are obtained.

3.2.2. Behaviour of $\bar{P}(\xi, I_K)$ in the neighbourhood of $\xi = \xi_{\max}$. We recall that $\xi_{\max}$ is defined as the maximum value of $\frac{mn(m)}{\mathcal{A}}$, which occurs at m_0, where $n(m_0) + m_0 n'(m_0) = 0$. Thus, in the neighbourhood of m_0 we can approximate $n(m) \sim n_0 - \frac{n_0}{m_0}(m - m_0)$, where $n_0 = n(m_0) = \frac{\mathcal{A}\xi_{\max}}{m_0}$ (the non-existence of other critical points is guaranteed by the twist condition). With this approximation, the argument of the δ function in (39) is quadratic in m. The integrations over m and $\mathcal{E}$ have to be carried out with attention to the requirement that the support of δ remains within the integration range. After some lengthy but straightforward manipulations, one gets

$$\bar{P}(\xi, I_K) \sim \frac{2}{gK\eta_{\max}} \int_{\sqrt{\frac{1}{(1+g)K\eta_{\max}}}}^{\sqrt{\frac{1}{K\eta_{\max}}}} \Theta\left(y - \frac{\zeta}{2}\right) \frac{y^{-3}\,\mathrm{d}y}{\sqrt{y^2 + 2y - \zeta}} \tag{58}$$

and

$$\eta_{\max} = \frac{(4n_0)^2}{2\mathcal{A}}, \qquad \zeta = \frac{\xi - \xi_{\max}}{\xi_{\max}}. \tag{59}$$

$\eta_{\max}$ is another dimensionless parameter which characterizes $\bar{P}(\xi, I_K)$ near the borders of its support. Performing the integral, we get

$$\begin{aligned}
\bar{P}(\xi, I_K) &\sim \frac{1}{gK\eta_{\max}}(F(y^{\uparrow}, \zeta) - F(y_{\downarrow}, \zeta)),\\
F(y, \zeta) &= \left(\frac{1}{\zeta y^2} + \frac{3}{\zeta^2 y}\right)\sqrt{y^2 + 2y - \zeta}\\
&\quad + \left(\frac{1}{\zeta} + \frac{3}{\zeta^2}\right)\begin{cases} \frac{-1}{\sqrt{|\zeta|}}\operatorname{arctanh}\frac{|\zeta|+y}{\sqrt{|\zeta|}\sqrt{y^2+2y-\zeta}} & \zeta \leqslant 0\\ \frac{1}{\sqrt{\zeta}}\arctan\frac{-\zeta+y}{\sqrt{\zeta}\sqrt{y^2+2y-\zeta}} & \zeta > 0, \end{cases}
\end{aligned} \tag{60}$$

$$y^{\uparrow} = \sqrt{\frac{1}{K\eta_{\max}}}, \qquad y_{\downarrow} = \sqrt{\frac{1}{(1+g)K\eta_{\max}}} \qquad \text{for} \quad \zeta \leqslant 0,$$

$$y^{\uparrow} = \sqrt{\frac{1}{K\eta_{\max}}}, \qquad y_{\downarrow} = \max\left\{\frac{\zeta}{2}, \sqrt{\frac{1}{(1+g)K\eta_{\max}}}\right\} \qquad \text{for} \quad \zeta > 0.$$

This expression includes the corrections to the limit distribution at its most noticeable feature, namely its singularity at $\xi_{\max}$. For finite K, the square-root singularity is replaced by a continuous function which reaches beyond $\xi_{\max}$, shifts the maximum from $\xi_{\max}$ to $\xi_{\max}(K, g) = \xi_{\max} + 2\sqrt{\frac{1}{(1+g)K\eta_{\max}}}$ and extends the support of $P(\xi, I_K)$ up to $\xi_{\max} + 2\sqrt{\frac{1}{K\eta_{\max}}}$. As $K \to \infty$, the expression converges to the limit. The applications of the above theory for an ellipsoid of revolution for two values of K are shown in figures 5 and 6.

3.2.3. Behaviour of $\bar{P}(\xi, I_K)$ in the neighbourhood of $\xi = 0$. In the neighbourhood of $\xi = 0$ we have contributions from the support of the delta function in (39) from the neighbourhood of $m = 0$, provided that $(m + \delta m)_- > \frac{1}{2\sqrt{\mathcal{E}}}$, and $m = m_{\max}$, provided that

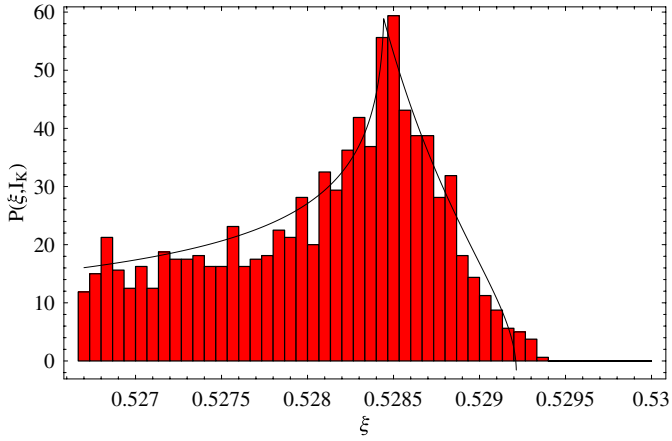

Figure 5. Local behaviour of $P(\xi, I_K)$ at $\xi = \xi_{\max}$ for an ellipsoid of revolution with eccentricity $\varepsilon = 0.5$ ($K = 24\,000$ and $g = 1$).

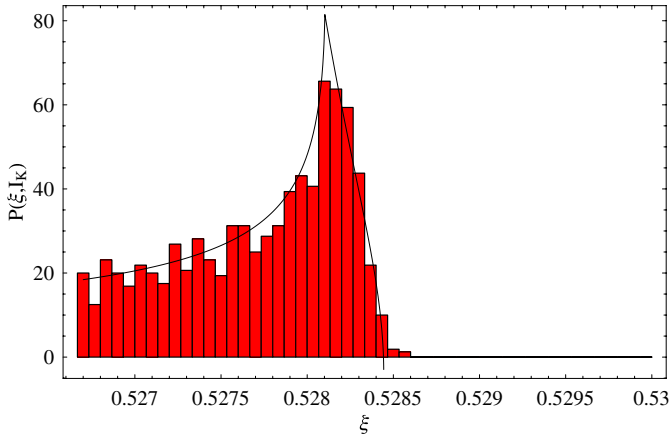

Figure 6. Local behaviour of $P(\xi, I_K)$ at $\xi = \xi_{\max}$ for an ellipsoid of revolution with eccentricity $\varepsilon = 0.5$ ($K = 48\,000$ and $g = 0.5$).

$\xi > \frac{1}{\mathcal{A}}\left(mn(m) + \frac{m}{2\sqrt{\varepsilon}}\right)_{m_{\max}}$. Putting all contributions together, we have

$$\bar{P}(\xi, I_K) \sim \frac{1}{2}\begin{cases} 0 & \text{for} \quad 0 < \xi \leqslant \sqrt{\dfrac{\eta_-}{K(1+g)}} \\ \dfrac{1}{g}\dfrac{1}{1-\xi/\eta_-}\left[(1+g) - \dfrac{\eta_-}{K\xi^2}\right] & \text{for} \quad \sqrt{\dfrac{\eta_-}{K(1+g)}} < \xi \leqslant \sqrt{\dfrac{\eta_-}{K}} \\ \dfrac{1}{1-\xi/\eta_-} & \text{for} \quad \sqrt{\dfrac{\eta_-}{K}} < \xi \end{cases}$$
$$+\frac{1}{2}\begin{cases} 0 & \text{for} \quad 0 < \xi \leqslant \sqrt{\dfrac{\eta_0}{K(1+g)}} \\ \dfrac{1}{g}\dfrac{1}{1-\xi/\eta_+}\left[(1+g) - \dfrac{\eta_0}{K\xi^2}\right] & \text{for} \quad \sqrt{\dfrac{\eta_0}{K(1+g)}} < \xi \leqslant \sqrt{\dfrac{\eta_0}{K}} \\ \dfrac{1}{1-\xi/\eta_+} & \text{for} \quad \sqrt{\dfrac{\eta_0}{K}} < \xi. \end{cases} \tag{61}$$

The most important feature in (61) is that it shifts the support of $\bar{P}(\xi, I_K)$ away from $\xi = 0$ to $\min\left\{\sqrt{\frac{\eta_-}{K(1+g)}}, \sqrt{\frac{\eta_0}{K(1+g)}}\right\}$. Note that most of the expressions which make up $P(\xi, I_K)$ in the neighbourhood of $\xi = 0$ are confined to a ξ interval of size $O\left(\frac{1}{\sqrt{K}}\right)$. Beyond this interval $\left(\frac{1}{\sqrt{K}} \ll \xi < \xi_{\max}\right)$ $P(\xi, I_K)$ takes the form

$$P(\xi, I_K) \sim \frac{1}{2}\left(\frac{1}{1-\frac{\xi}{\eta_-}} + \frac{1}{1-\frac{\xi}{\eta_+}}\right), \tag{62}$$

which coincides with the small ξ expression of the limit distribution (46) to leading order in ξ. To obtain the dominant behaviour of $P(\xi, I_K)$ near $\xi = 0$, one should add $P_{m=0}(\xi, I_K)$ which we compute now.

3.2.4. The contribution of the $m = 0$ term in (30). Following the same steps as above, the leading approximation to $P_{m=0}(\xi, I_K)$ reads

$$P_{m=0}(\xi, I_K) \sim \frac{1}{gK}\int_{-\frac{1}{2}}^{\infty} \chi_{I_K}\left(2\mathcal{A}H\left(n+\frac{1}{2}, 0\right)\right)\delta\left(\xi - \frac{n+1}{2\mathcal{A}H\left(n+\frac{1}{2}, 0\right)}\right)\mathrm{d}n. \tag{63}$$

This being already a correction term, we are allowed to neglect the semi-classical correction $\frac{1}{2}$ to n in the argument of $H\left(n+\frac{1}{2}, 0\right)$. With $H(n, 0) = \left(\frac{\pi n}{\mathcal{L}}\right)^2$ from (20), we get

$$P_{m=0}(\xi, I_K) \sim \frac{1}{gK}\int_{\frac{\mathcal{L}}{\pi}\sqrt{\frac{K}{2\mathcal{A}}}}^{\frac{\mathcal{L}}{\pi}\sqrt{\frac{K(1+g)}{2\mathcal{A}}}} \delta\left(\xi - \frac{1}{n}\frac{\mathcal{L}^2}{2\mathcal{A}\pi^2}\right)\mathrm{d}n. \tag{64}$$

Therefore,

$$P_{m=0}(\xi, I_K) \sim \begin{cases} \dfrac{1}{\xi^2}\dfrac{\eta_-}{gK} & \text{if } \sqrt{\dfrac{\eta_-}{K(1+g)}} \leqslant \xi < \sqrt{\dfrac{\eta_-}{K}} \\ 0 & \text{otherwise,} \end{cases} \tag{65}$$

where η_- is defined in (47). Both the shift of the support away from the origin $\xi = 0$ and its size decrease as $\frac{1}{\sqrt{K}}$. In its support, $P_{m=0}(\xi, I_K)$ is bounded between the values $\frac{1}{g}$ and $1 + \frac{1}{g}$. However, although the contribution of this term to the probability density is $O(1)$, its effect on the probability is $O\left(\frac{1}{K}\right)$, or in other words, $P_{m=0}(\xi, I_K) = O\left(\frac{1}{K}\right)$ in the weak sense. In this vicinity, $P_{m=0}(\xi, I_K)$ depends only on a single geometric parameter, η_-. Note that *a priori*, one would have expected the lower limit of the support of $\bar{P}(\xi, I_K)$ to be $O\left(\frac{1}{K}\right)$, and not $O\left(\frac{1}{\sqrt{K}}\right)$. This prediction stems from the definition of the normalized nodal sequence (26); for $\mathcal{N} > 1$ we have the lower bound $\xi_{\mathcal{N}} \geqslant \frac{2}{\mathcal{N}}$, so $P(\xi, I_K) \equiv 0$ for $\xi < \frac{2}{(1+g)K}$, and not for $\xi < O\left(\frac{1}{\sqrt{K}}\right)$ as observed.

The oscillatory terms $Q(I_K)$ contribute terms of order $\frac{1}{\sqrt{K}}$ in the $\xi = 0$ vicinity. They originate from a Gibbs phenomenon and will be discussed in appendix B. Figures 6 and 7 compare the results of numerical simulations with the expressions derived above in the vicinity of $\xi = 0$, and the theory includes also the oscillatory corrections (to be precise, with the integrated density $\Pi(\xi, I_K) := \int_0^{\xi} P(\xi', I_K)\,\mathrm{d}\xi'$).

The deviations of the theory from the numerical data in figures 5–8 are due to (i) the sensitivity of the features of the distribution in the $\xi = 0$ and $\xi = \xi_{\max}$ regions (e.g. the extent of its support) to $O\left(\frac{1}{\sqrt{K}}\right)$ errors, (ii) statistical error-bin size versus resolution and (iii) the approximation used for the oscillatory part discussed in appendix B. All are justifiable for the size of the spectral data set used.

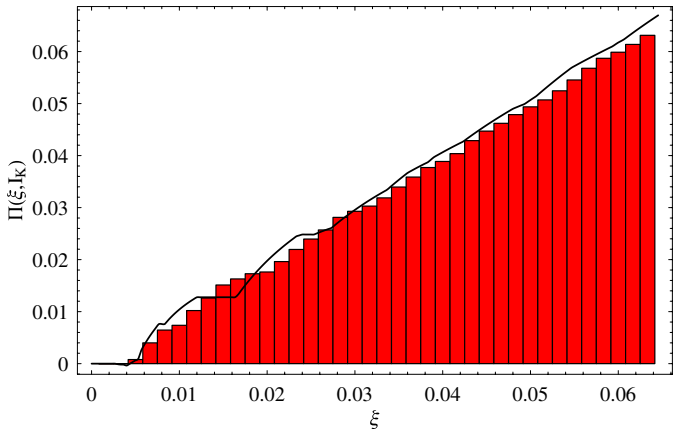

Figure 7. Local behaviour of $\Pi(\xi, I_K)$ at $\xi = 0$ for an ellipsoid of revolution with eccentricity $\varepsilon = 0.5$ ($K = 24\,000$, $g = 1$).

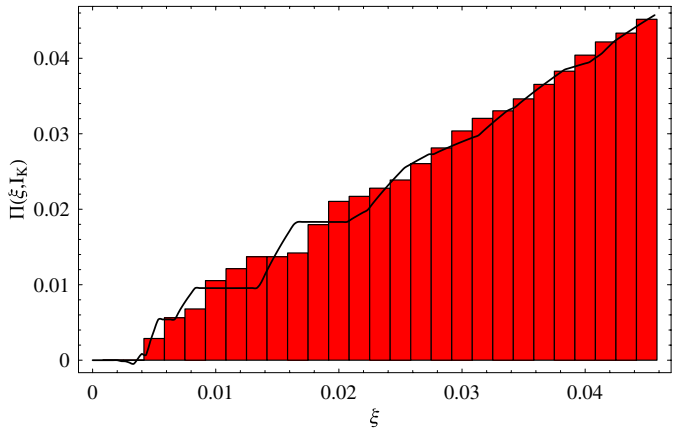

Figure 8. Local behaviour of $\Pi(\xi, I_K)$ at $\xi = 0$ for an ellipsoid of revolution with eccentricity $\varepsilon = 0.5$ ($K = 48\,000$, $g = 0.5$).

3.3. The oscillatory contributions $Q(\xi, I_K)$

3.3.1. Weak estimate of $Q(I_K)$. In this section we estimate the oscillatory part $Q(\xi, I_K)$, defined in (32). We show that it is of smaller order in $\frac{1}{\sqrt{K}}$ than the leading order correction of the corresponding smooth part. This justifies the preceding analysis where we considered only the smooth part, which gives the only contribution of $O\left(\frac{1}{\sqrt{K}}\right)$. The numerical results also give evidence of this self-averaging process in the semi-classical limit.

To be more precise, we shall show that

$$\int_0^1 Q(\xi, I_K)\varphi(\xi)\mathrm{d}\xi = o\left(\frac{1}{K}\right) \tag{66}$$

for any test function φ. We shall follow a series of natural regularizations which are justified in studying this weak limit. We shall also discuss the local behaviour of $Q(\xi, I_K)$ in the neighbourhood of $\xi = 0$, in order to compare with the numerical results.

We have $Q(\xi, I_K) = \sum_{(N,M)\neq 0} Q_{N,M}(\xi, I_K)$, where the Fourier components (33) are approximated as

$$Q_{N,M}(\xi, I_K) \sim \frac{1}{gK}\int_{K/2\mathcal{A}}^{(1+g)K/2\mathcal{A}} \mathrm{d}\mathcal{E} \int_0^{m_{\max}} \delta\left(\xi - \frac{mn(m)}{\mathcal{A}}\right) |n(m) - mn'(m)| \mathrm{e}^{2\pi \mathrm{i}\sqrt{\mathcal{E}}(Mm+Nn(m))}\,\mathrm{d}m. \tag{67}$$

We now turn to a smoothing of this distribution by adding a small imaginary part to the argument of the delta function, say $\varepsilon > 0$. This amounts to replacing the δ function by the Lorentzian

$$\delta^{\varepsilon}(\xi) = 2\mathrm{Re}\int_0^{\infty} \mathrm{e}^{2\pi \mathrm{i}\xi x}\mathrm{e}^{-2\pi\varepsilon x}\,\mathrm{d}x = \frac{1}{\pi}\frac{\varepsilon}{\varepsilon^2+\xi^2}. \tag{68}$$

And so,

$$Q^{\varepsilon}_{N,M}(\xi, I_K) \sim \frac{\varepsilon}{\pi g K}\int_{K/2\mathcal{A}}^{(1+g)K/2\mathcal{A}} \frac{\mathrm{e}^{2\pi \mathrm{i}\sqrt{\mathcal{E}}(Mm+Nn(m))}}{\varepsilon^2 + (\xi - \xi_{n(m),m})^2}|n(m) - mn'(m)|\mathrm{d}m. \tag{69}$$

We must note here a qualitative difference between the semi-classical theory of the spectral density and the nodal domain distribution. The index set $I_K = [K, K + \Delta K]$ corresponds to a spectral interval $[E_K, E_{K+\Delta K}]$. In the later case, as $K \to \infty$, the eigenvalues are distributed in an ever-growing interval, while the normalized nodal sequence is distributed in $(0, 1]$, becoming arbitrarily dense. So, in contrast to the regularization of the spectral density, in general we do not expect the limits $\varepsilon \to 0+$ and $K \to \infty$ to commute for the nodal domain distribution. We shall first consider the semi-classical limit.

Once again, by the linear approximation, we have $n(m) = n_{\pm} + n'_{\pm}(m - m_{\pm}) + O\left(\frac{1}{\sqrt{\mathcal{E}}}\right)$, and $mn(m)/\mathcal{A} = \frac{1}{\mathcal{A}}(n_{\pm} + m_{\pm}n'_{\pm})(m - m_{\pm}) + O\left(\frac{1}{\sqrt{\mathcal{E}}}\right) =: \xi'_{\pm}(m - m_{\pm}) + O\left(\frac{1}{\sqrt{\mathcal{E}}}\right)$.

By taking the whole real line as the m-integration range and shifting $m \mapsto x = m - m_{\sigma}$ ($\sigma = \pm$), we have

$$\begin{aligned} Q^{\varepsilon}_{N,M}(\xi, I_K) &\sim \sum_{\sigma=\pm}\frac{\varepsilon}{\pi g K}(n_{\sigma} - m_{\sigma}n'_{\sigma})\int_{K/2\mathcal{A}}^{(1+g)K/2\mathcal{A}} \mathrm{d}\mathcal{E}\,\mathrm{e}^{2\pi \mathrm{i}S\sqrt{\mathcal{E}}}\int_{-\infty}^{\infty}\frac{\mathrm{e}^{2\pi\mathrm{i}\sqrt{\mathcal{E}}Rx}}{\varepsilon^2 + (\xi - \xi'_{\sigma}x)^2}\,\mathrm{d}x \\ &= \sum_{\sigma}\frac{1}{gK}\frac{n_{\sigma} - m_{\sigma}n'_{\sigma}}{n_{\sigma} + m_{\sigma}n'_{\sigma}}\int_{K/2\mathcal{A}}^{(1+g)K/2\mathcal{A}} \mathrm{e}^{2\pi\mathrm{i}S\sqrt{\mathcal{E}} - 2\pi\varepsilon\sqrt{\mathcal{E}}|\frac{R}{\xi'_{\sigma}}|}\,\mathrm{d}\mathcal{E} \\ &= \sum_{\sigma}\frac{2}{gK}\frac{n_{\sigma} - m_{\sigma}n'_{\sigma}}{n_{\sigma} + m_{\sigma}n'_{\sigma}}\int_{\sqrt{K/2\mathcal{A}}}^{\sqrt{(1+g)K/2\mathcal{A}}} \mathrm{e}^{2\pi(\mathrm{i}S - \varepsilon|\frac{R}{\xi'_{\sigma}}|)k}k\,\mathrm{d}k, \end{aligned} \tag{70}$$

with

$$\begin{pmatrix} R \\ S \end{pmatrix} = \begin{pmatrix} n'_{\sigma} & 1 \\ n_{\sigma} & m_{\sigma} \end{pmatrix}\begin{pmatrix} N \\ M \end{pmatrix}.$$

Now, instead of a sharp uniform window (taking into account only those states whose index lie in the interval I_K), we consider a Gaussian regularization

$$h_K(k) = \frac{1}{\sqrt{\pi}v}\exp(-(k-\mu)^2/v^2), \tag{71}$$

with $\mu = \frac{\sqrt{1+g}+1}{2}\sqrt{\frac{K}{2\mathcal{A}}}$ and $v = (\sqrt{1+g} - 1)\sqrt{\frac{K}{2\mathcal{A}}}$, and extend the integration over the whole real line (of course, this regularization does not affect the asymptotic behaviour we study):

$$Q^{\varepsilon}_{N,M}(\xi, I_K) \sim \sum_{\sigma=\pm}\frac{2}{\sqrt{\pi}vgK}\frac{n_{\sigma} - m_{\sigma}n'_{\sigma}}{n_{\sigma} + m_{\sigma}n'_{\sigma}}\int_{-\infty}^{\infty} \mathrm{e}^{2\pi(\mathrm{i}S - \varepsilon|\frac{R}{\xi'_{\sigma}}|)k - (k-\mu)^2/v^2}k\,\mathrm{d}k$$

$$= \sum_{\sigma} \frac{2}{\sqrt{\pi} v g K} \frac{n_\sigma - m_\sigma n'_\sigma}{n_\sigma + m_\sigma n'_\sigma} \mathrm{e}^{-\mu^2/v^2} \int_{-\infty}^{\infty} \mathrm{e}^{-k^2/v^2 + (2\pi \mathrm{i} S - 2\pi\varepsilon |\frac{R}{\xi'_\sigma}| + 2\mu/v^2)k} k \, \mathrm{d}k$$

$$= \sum_{\sigma} \frac{2v^2}{gK} \frac{n_\sigma - m_\sigma n'_\sigma}{n_\sigma + m_\sigma n'_\sigma} \left(\pi \mathrm{i} S - \pi \varepsilon \left| \frac{R}{\xi'_\sigma} \right| + \frac{\mu}{v^2} \right)$$

$$\times \exp\left(-\pi^2 v^2 S^2 + \pi^2 \varepsilon^2 v^2 \frac{R^2}{\xi'^2_\sigma} - 2\pi^2 \mathrm{i} \varepsilon v^2 \left| \frac{R}{\xi'_\sigma} \right| S + 2\mu\pi \mathrm{i} S - 2\pi\mu\varepsilon \left| \frac{R}{\xi'_\sigma} \right| \right). \quad (72)$$

We proceed towards a crude, yet sufficient for our purpose, estimate for $Q(\xi, I_K)$,

$$|Q_\varepsilon(\xi, I_K)| \leqslant \sum_{(N,M)\neq 0} \sum_{\sigma=\pm} \frac{2v^2}{gK} \left| \frac{n_\sigma - m_\sigma n'_\sigma}{n_\sigma + m_\sigma n'_\sigma} \right| \left(\pi |S| + \pi \varepsilon \left| \frac{R}{\xi'_\sigma} \right| + \frac{\mu}{v^2} \right)$$

$$\times \exp\left(-\pi^2 v^2 S^2 + \pi^2 \varepsilon^2 v^2 \frac{R^2}{\xi'^2_\sigma} - 2\pi\mu\varepsilon \left| \frac{R}{\xi'_\sigma} \right| \right). \quad (73)$$

By taking into account that $\sum_{\gamma\in\mathbb{Z}^2} \mathrm{e}^{-t(\alpha\cdot\gamma)^2 + \sqrt{t}\beta\cdot\gamma} \asymp \frac{1}{t}$ and $\sum_{\gamma\in\mathbb{Z}^2} |\gamma^i| \mathrm{e}^{-t(\alpha\cdot\gamma)^2+\sqrt{t}\beta\cdot\gamma} \asymp \frac{1}{t^{3/2}}$, $t \to \infty$, we have

$$|Q_\varepsilon(\xi, I_K)| \leqslant O\left(\frac{1}{K^{3/2}} \right) \quad (74)$$

uniformly in ε (before the limit $\varepsilon \to 0+$ is taken, all three terms in the amplitude of the summed quantity contribute to this same order; $\frac{\mu}{v^2} \asymp \frac{1}{\sqrt{K}}$).

3.3.2. Local estimate of $Q(\xi, I_K)$ in the neighbourhood of $\xi = 0$. From the numerical investigations, a clear oscillatory behaviour of the distribution is observed in the neighbourhood of $\xi = 0$, which implies the importance of the oscillatory part in that region. This is due to a Gibbs phenomenon, and is not in contradiction to the fact that the oscillatory part $Q(I_K)$ is of less order in the weak sense than the smooth part $\bar{P}(I_K)$—this is a local contribution.

We find the manifestation in the dominant terms $\sum_N Q_{N,0}$ and $\sum_M Q_{0,M}$, which agrees with the numerical results. The explicit form of these contributions are presented in appendix B.

4. The geometric information stored in the nodal sequence

The derivation of the probability density $P(\xi, I_K)$ in the preceding section is based on functions which are obtained directly from the dynamical relations embedded in the Hamiltonian and its dependence on the action variables. These, in turn, are computed from the profile curve $y = f(x)$, which defines $\mathcal{M}$. Here, we would like to investigate the possibility of inverting this relationship, and ask what can be said about the surface once the nodal sequence is known.

A few parameters can be easily extracted from the probability density $P(\xi, I_K)$. Taking the limit $K \to \infty$ we get the limit distribution $P(\xi)$. Its support provides the parameter $\xi_{\max}$. In the vicinity of $\xi = 0$, $P(\xi)$ depends symmetrically on the two parameters η_- and η_+. This provides a useful relationship, which can be combined with the information from $P(\xi, I_K)$ near $\xi = 0$, for finite K, which depends on all four (independent) geometric parameters, η_-, η_+, η_0 and $\eta_{\max}$. These parameters are related to the geometry of surface (47).

There are further reasons to extract the parameters $\{\eta_-, \eta_+, \eta_0, \eta_{\max}\}$. First, these parameters encapsulate the characteristic local features of the limiting distribution $P(\xi)$ and the various contributions to the semi-classical nodal distribution $P(\xi, I_K)$, even for the non-mirror-symmetric $\mathcal{M}$. This gives a basis for a computational approach to the scheme put

forward: given a set of spectral data with sufficiently large K, the nodal domain distribution can be constructed, and thus the geometric parameters can be recovered by a best-fit procedure in the appropriate regimes of ξ. Second, the parameters are needed in the final step of the nodal inversion algorithm, as will be made clear in what follows.

As was commented in the previous section, relations (44) and (57) can be solved to obtain the two branches $m_-(\xi)$ and $m_+(\xi)$. Consequently, the function $n(m)$ is determined, since $n(m_\pm(\xi)) = \frac{\mathcal{A}\xi}{m_\pm(\xi)}$. This will be the first step towards the inversion of the nodal counting data which will be explained in the following subsection.

4.1. Inversion of the nodal sequence

In this section we discuss nodal domain inversion in detail. The first result is: *with the distribution $\bar{P}(I_K)$ as given data, the 'scale-invariant' action $n(m)/\sqrt{\mathcal{A}}$ is determined uniquely.* For simple surfaces of revolution (separable systems in general with the Hamiltonian satisfying the homogeneity condition), $n(m)$ incorporates all the information about the dynamics, and as we shall see in some cases, the actual geometry.

Our starting point is the semi-classical asymptotic expansion (52),

$$\bar{P}(\xi, I_K) \sim P(\xi) + \frac{1}{\sqrt{K}} P_1(\xi), \tag{75}$$

which, for convenience, we solve for $P_1(\xi)$,

$$P_1(\xi) = \sqrt{K}(\bar{P}(\xi, I_K) - P(\xi)) + O\left(\frac{1}{\sqrt{K}}\right). \tag{76}$$

Obviously, P and P_1 are determined from the given data,

$$\lim_{K\to\infty} \bar{P}(I_K) = P \qquad \text{and} \qquad \lim_{K\to\infty} \sqrt{K}(\bar{P}(I_K) - P) = P_1. \tag{77}$$

From relation (44),

$$P(\xi) = \xi \frac{\mathrm{d}}{\mathrm{d}\xi} \log \frac{m_-(\xi)}{m_+(\xi)} \Rightarrow \frac{m_+(\xi)}{m_-(\xi)} = \exp \int_\xi^{\xi_{\max}} \frac{P(\xi')}{\xi'} \mathrm{d}\xi', \tag{78}$$

the ratio $m_+(\xi)/m_-(\xi)$ is determined, given P. Accompanying the above, we have relation (57),

$$P_1(\xi) = -\sqrt{\frac{2}{\mathcal{A}}} \frac{\sqrt{1+g}-1}{g} \sqrt{\xi} \frac{\mathrm{d}}{\mathrm{d}\xi} \left(\sqrt{\xi} \frac{\mathrm{d}}{\mathrm{d}\xi} [m_+(\xi) - m_-(\xi)] \right), \tag{79}$$

which can be inverted to give

$$u(\xi) := \frac{1}{\sqrt{\mathcal{A}}}(m_+(\xi) - m_-(\xi)) = -\frac{1}{\sqrt{2}} \frac{g}{\sqrt{1+g}-1} \int^\xi \frac{1}{\sqrt{\xi'}} \left(\int^{\xi'} \frac{P_1(\xi'')}{\sqrt{\xi''}} \mathrm{d}\xi'' \right) \mathrm{d}\xi'. \tag{80}$$

To determine $u(\xi)$ uniquely, two integration constants should be provided, and they are given in terms of the initial conditions for $u(\xi)$ and $\frac{\mathrm{d}u(\xi)}{\mathrm{d}\xi}$ at the point $\xi = 0$ or $\xi = \xi_{\max}$. They are expressed in terms of the geometric parameters $\{\eta_-, \eta_+, \eta_0, \eta_{\max}\}$, which are extracted from the form of $P(\xi)$ near $\xi = 0$ and $\xi = \xi_{\max}$. Thus, the ratio and the difference between $m_+(\xi)$ are $m_-(\xi)$ are given. Together with $n_\pm(\xi) = \xi \frac{\mathcal{A}}{m_\pm(\xi)}$, they give the parametric representation of Γ. Note that we require no information from the statistical properties of the nodal counts of the isotropic quantum states, i.e. $P_{m=0}(I_K)$.

The significance of this result becomes apparent in the following section, where we confine ourselves to mirror-symmetric surfaces.

4.2. Mirror-symmetric $f(x)$ is uniquely determined by $n(m)$

Following the preceding section, we prove that if the generating curve f is mirror-symmetric (i.e. $f(-x) = f(x)$) the action variable $n(m)$ determines f uniquely.

Since f is an even function, we may write

$$n(m) = \frac{2}{\pi}\int_0^{x_+} \sqrt{f(x)^2 - m^2}\,\frac{\sqrt{1+f'(x)^2}}{f(x)}\,\mathrm{d}x, \tag{81}$$

where $f(x_+) = m$, or $x_+ = f^{-1}(m)$. Changing the variable $x \mapsto u = f(x)/m_{\max}$,

$$n(m) = \frac{2}{\pi}\int_{m/m_{\max}}^1 \frac{\sqrt{m_{\max}^2u^2 - m^2}}{u}\,\frac{\sqrt{1+f'\circ f^{-1}(m_{\max}u)^2}}{|f'\circ f^{-1}(m_{\max}u)|}\,\mathrm{d}u. \tag{82}$$

Suppose that f, g are different curves of this class which give the same action variable, i.e.

$$\begin{aligned}\int_{m/m_{\max}(f)}^1 &\frac{\sqrt{m_{\max}(f)^2u^2 - m^2}}{u}\,\frac{\sqrt{1+f'\circ f^{-1}(m_{\max}(f)u)^2}}{|f'\circ f^{-1}(m_{\max}(f)u)|}\,\mathrm{d}u \\ &= \int_{m/m_{\max}(g)}^1 \frac{\sqrt{m_{\max}(g)^2u^2 - m^2}}{u}\,\frac{\sqrt{1+g'\circ g^{-1}(m_{\max}(g)u)^2}}{|g'\circ g^{-1}(m_{\max}(g)u)|}\,\mathrm{d}u,\end{aligned} \tag{83}$$

while $f \neq g$.

First, note that $m_{\max}(f) = m_{\max}(g)$. This is because $m_{\max}$ is the sole real root of $n(m)$, thus, since both sides of the above equality are proportional to $n(m)$ they must have a common root, denoted simply be $m_{\max}$, since $n(m)$ is analytic on $(0, m_{\max}]$. Thus, since the integration limits are identical, the integrands must be equal.

It suffices to show that $\frac{\sqrt{1+f'\circ f^{-1}(y)^2}}{|f'\circ f^{-1}(y)|} = \frac{\sqrt{1+g'\circ g^{-1}(y)^2}}{|g'\circ g^{-1}(y)|}$, for $y \in [0, m_{\max}]$, implies $f = g$. From the above we have $f'\circ f^{-1}(y) = g'\circ g^{-1}(y)$. The problem has been reduced to showing that the nonlinear operator $Af = f'\circ f^{-1}$ acting on our function class possesses an inverse, i.e. $Af = Ag \Leftrightarrow f = g$.

Consider the inhomogeneous 'functional' equation $f'\circ f^{-1} = h$, for some h in some other appropriate function class. We shall show that for a given h, this determines, along with some initial condition, a unique f, formally $f = A^{-1}h$. We have $f'(f^{-1}(y)) = h(y)$, or $f'(x) = h(f(x))$, since $y = f(x)$. Thus, we have reduced this to a first-order ordinary differential equation, $y' = h(y)$. Accompanied by the initial condition $f(0) = m_{\max}$, this becomes an initial value problem on $[0, 1]$ with a unique solution (h is smooth on $[0, 1)$). Thus, A^{-1} exists and is unique.

In our problem, the initial condition is provided by knowledge of the root of $n(m)$, so we have reached the conclusion that the two integrals cannot equal if $f \neq g$.

5. Summary and conclusions

The unique inversion of the nodal sequence which was demonstrated above for symmetric and 'simple' surfaces of revolution paves the way to a sequence of problems which should now be addressed. Other families of compact separable manifolds are known, amongst which the Liouville surfaces [18] and the axially symmetric Zoll surfaces [19] are of prime importance. We believe that the general approach taken in the present paper could be applied to handle these cases, however, modifications should be applied to take care of special problems which are intrinsic to these systems, and this remains for a further study. Another class of integrable/separable systems consists of independent particle models which are commonly

used in atomic and nuclear physics. The study of such systems extends the research of nodal domains to systems with arbitrary dimensions.

The next systems in complexity are systems which are classically integrable but are not separable quantum mechanically. The simplest examples consist of, e.g., the Dirichlet Laplacians in the equilateral or the isosceles right triangular domains. Even though the spectrum can be expressed precisely in terms of the 'quantum numbers', counting of nodal domains is difficult, and the study of the nodal sequences in such cases might call for other approaches than the one pursued here.

Do nodal sequences in other systems store geometric information? Is there a way to extract this information to determine the geometry? These are yet open problems, and the only hint for an affirmative answer comes from preliminary numerical simulations which indicate that 'nodal' trace formulae exist for 'quantum graphs' [11] and for 'chaotic billiards' [20]. No rigorous treatment exists so far.

Acknowledgments

The authors would like to thank Professor Jon Keating and Dr Sven Gnutzmann for lengthy and enlightening discussions. This work was supported by the Minerva Center for Nonlinear Physics and the Einstein (Minerva) Center at the Weizmann Institute, by the ISF and grants from the GIF (grant I-808-228.14/2003) and EPSRC (grant GR/T06872/01).

Appendix A. The regularization of the action integral

The action variable (5) is defined in terms of an integral, whose form is not convenient for further computations, such as, e.g., the evaluation of its higher derivatives. This can be done by regularizing the integral in a way which will be explained here. Rather than introducing fractional derivatives as was done in, e.g. [15], we compute the integrals explicitly. It is convenient to introduce the notations $q(x) = f(x)^2$ and $\mu = m^2$. We start with

$$n(\mu) = \frac{1}{\pi}\int_{x_-}^{x_+} \sqrt{q(x)-\mu}\,\frac{\sqrt{4q(x)+q'(x)^2}}{2q(x)}\,\mathrm{d}x, \qquad \text{where} \quad q(x_\pm) = \mu. \tag{A.1}$$

The function $q(x)$ is analytic in I and has a single maximum at $x_{\max}$. We separate the integration interval in (A.1) to two consecutive intervals $[x_-, x_{\max}]$ and $[x_{\max}, x_+]$ and write accordingly

$$n(\mu) = n_-(\mu) + n_+(\mu). \tag{A.2}$$

In each of the intervals $[-1, x_{\max})$ and $(x_{\max}, 1]$, $q(x)$ is a monotonic function. Therefore, it can be inverted in each of the intervals in terms of the corresponding functions $x_\pm(q)$, which are analytic in the interval $[0, q_{\max})$. Thus,

$$n_\pm(\mu) = \frac{1}{\pi}\int_{\mu}^{q_{\max}} \sqrt{q-\mu}\,w_\pm(q)\,\mathrm{d}q, \tag{A.3}$$

with

$$w_\pm(q) = \frac{1}{2q}\sqrt{4q\left(\frac{\mathrm{d}x_\pm(q)}{\mathrm{d}q}\right)^2 + 1}. \tag{A.4}$$

The expression in the above square root is analytic in the domain of q where $x_\pm(q)$ are analytic, that is, in $[0, q_{\max})$. They can be Taylor expanded with a convergence radius $q_{\max}$ so that

$$w_\pm(q) = \frac{1}{2q} + \sum_{r=0}^{\infty} \tau_r^\pm q^r. \tag{A.5}$$

Substituting these expressions in (A.3), performing the integrals and defining $\tau_r = \tau_r^+ + \tau_r^-$, we finally get

$$n(\mu) = \frac{2}{\pi}\left[(q_{\max}-\mu)^{\frac{1}{2}} - \mu^{\frac{1}{2}}\arccos\left(\frac{\mu}{q_{\max}}\right)^{\frac{1}{2}}\right] + \frac{1}{\pi}\sum_{r=0}^{\infty}\tau_r I_r(\mu), \tag{A.6}$$

where

$$I_r(\mu) = \int_{\mu}^{q_{\max}} q^r\sqrt{q-\mu}\,\mathrm{d}q = (q_{\max}-\mu)^{\frac{3}{2}}\sum_{k=0}^{r}\binom{r}{k}\frac{(q_{\max}-\mu)^{r-k}\mu^k}{(r-k)+\frac{3}{2}}. \tag{A.7}$$

Using (7) we find

$$n(0) = \frac{\mathcal{L}}{\pi} = \frac{1}{\pi}\sqrt{q_{\max}}\left[2+\sum_{r=0}^{\infty}\frac{\tau_r q_{\max}^{r+1}}{r+\frac{3}{2}}\right]. \tag{A.8}$$

Thus in the vicinity of $\mu = 0$, we get

$$n(\mu) \sim \frac{\mathcal{L}}{\pi} - \sqrt{\mu}. \tag{A.9}$$

The behaviour of $n(\mu)$ near the other extreme end of the interval, $\mu = q_{\max}$, cannot be deduced in the same way, because $x(q)$ is not defined at this point. However, starting directly from (A.1) we can obtain the behaviour of $n(\mu)$ in this domain. For this purpose, we write

$$q(x) \sim q_{\max} - \frac{1}{2}\omega(x-x_{\max})^2, \qquad \omega = |q''(x_{\max})|, \qquad x \to x_{\max}. \tag{A.10}$$

To leading order in $(q_{\max}-\mu)$, (A.1) reduces to

$$n(\mu) \sim \frac{2}{\pi\sqrt{2\omega q_{\max}}}\int_{\mu}^{q_{\max}}\sqrt{\frac{q-\mu}{q_{\max}-q}}\mathrm{d}q = \frac{q_{\max}-\mu}{\sqrt{2\omega q_{\max}}} \sim \sqrt{\frac{2}{\omega}}(f_{\max}-|m|). \tag{A.11}$$

Finally, we return to the example of the sphere. With $f(x)^2 = 1-x^2$ the integrals can be performed exactly,

$$n(m) = 1 - |m|. \tag{A.12}$$

This is consistent with the local expressions presented in (A.9) and (A.11).

Appendix B. The oscillatory part near the origin

We recover the oscillatory behaviour of the distribution near $\xi = 0$ from the leading order sums

$$Q(\xi, I_K) \sim \sum_{N\in\mathbb{Z}_*} Q_{N,0}(\xi, I_K) + \sum_{M\in\mathbb{Z}_*} Q_{0,M}(\xi, I_K). \tag{B.1}$$

We begin with (33). As $\xi \to 0+$, the contribution in the above integral will come from the neighbourhoods of $m = 0$ and $m = m_{\max}$ (the delta function of the integrand is supported on $\{m+\delta m\}_{\pm}$). These will be treated separately, denoted by $Q^{\pm}_{N,M}(\xi, I_K)$, respectively, so that

$$Q_{N,M}(\xi, I_K) = Q^-_{N,M}(\xi, I_K) + Q^+_{N,M}(\xi, I_K). \tag{B.2}$$

In what follows, we define $x := \xi/\eta_-$ when referring to the Q^- terms, and $x := \xi/\eta_+$ for the Q^+ terms.

Given that $m_- \sim \frac{\mathcal{L}}{2\pi}x$ and $\delta m_- \sim -\frac{1}{2}\eta x$, by changing variables to the appropriate dimensionless wave number $k := \mathcal{L}\sqrt{\mathcal{E}}$, we have

$$Q^-_{0,M}(\xi, I_K) \sim \frac{1}{\pi^2\eta_- g K}\frac{\mathrm{e}^{-\pi\mathrm{i}Mx/2}}{1-x}\int_{\pi\sqrt{\eta_- K}}^{\pi\sqrt{\eta_-(1+g)K}}\Theta\left(k-\frac{\pi}{x}\right)\mathrm{e}^{\mathrm{i}Mxk}\left(k-\frac{\pi}{2}\right)\mathrm{d}k. \tag{B.3}$$

Similarly, we carry out the calculation of the integral $Q^{+}_{0,M}(\xi, I_K)$. Here, the condition that $(m+\delta m)_+$ lies in the integration range reads $\mathcal{A}\xi > (mn(m)+\eta m)_{m_{\max}} = m_{\max}\eta$,

$$Q^{+}_{0,M}(\xi, I_K) \sim \frac{1}{\eta_0 g K}\frac{\mathrm{e}^{\pi \mathrm{i} M\sqrt{\omega/2}(1+x/2)}}{1-x}\int_{\sqrt{\eta_0 K}}^{\sqrt{\eta_0(1+g)K}} \times\Theta\left(k-\frac{1}{x}\right)\mathrm{e}^{2\pi \mathrm{i} M(1-x/2)k}\left(k-\frac{\sqrt{\omega/2}}{2}\right)\mathrm{d}k, \tag{B.4}$$

where the appropriate wave number is $k := m_{\max}\sqrt{\mathcal{E}}$.

Following the above calculations,

$$Q^{-}_{N,0}(\xi, I_K) \sim \frac{1}{\pi^2\eta_- g K}\frac{\mathrm{e}^{\pi \mathrm{i} N x/2}}{1-x}\int_{\pi\sqrt{\eta_- K}}^{\pi\sqrt{\eta_-(1+g)K}} \Theta\left(k-\frac{\pi}{x}\right)\mathrm{e}^{\mathrm{i}N(2-x)k}\left(k-\frac{\pi}{2}\right)\mathrm{d}k, \tag{B.5}$$

and

$$Q^{+}_{N,0}(\xi, I_K) \sim \frac{1}{\eta_0 g K}\frac{\mathrm{e}^{-\pi \mathrm{i} N(1+x/2)}}{1-x}\int_{\sqrt{\eta_0 K}}^{\sqrt{\eta_0(1+g)K}} \Theta\left(k-\frac{1}{x}\right)\mathrm{e}^{\pi \mathrm{i} N\sqrt{\omega/2}xk}\left(k-\frac{\sqrt{2/\omega}}{2}\right)\mathrm{d}k. \tag{B.6}$$

By performing the integrations, we have

$$\sum_{M\in\mathbb{Z}_*} Q_{0,M}(\xi, I_K) \sim \frac{1}{\pi\eta_- g K}\frac{1}{(1-x)x^2}\begin{cases} 0 & \text{for } \sqrt{\dfrac{\eta_-}{(1+g)K}} \geqslant \xi \\ f_1^-(\xi, I_K) & \text{for } \sqrt{\dfrac{1}{(1+g)\eta_- K}} < \xi \leqslant \sqrt{\dfrac{1}{\eta_- K}} \\ f_2^-(\xi, I_K) & \text{for } \sqrt{\dfrac{1}{\eta_- K}} < \xi \end{cases}$$
$$+\frac{1}{\pi\eta_0 g K}\frac{1}{(1-x)(2-x)^2}\begin{cases} 0 & \text{for } \sqrt{\dfrac{\omega}{2(1+g)\eta_0 K}} \geqslant \xi \\ f_1^+(\xi, I_K) & \text{for } \sqrt{\dfrac{\omega}{2\eta_0(1+g)K}} < \xi \leqslant \sqrt{\dfrac{\omega}{2\eta_0 K}} \\ f_2^+(\xi, I_K) & \text{for } \sqrt{\dfrac{\omega}{2\eta_0 K}} < \xi, \end{cases}$$

where

$$\begin{aligned} f_1^-(\xi, I_K) &:= \alpha\left(1-\frac{x}{2}\right) - \alpha\left(x\sqrt{\eta_- K}-\frac{x}{2}\right) + x\sqrt{\eta_- K}\beta\left(x\sqrt{\eta_- K}-\frac{x}{2}\right) - \beta\left(1-\frac{x}{2}\right), \\ f_2^-(\xi, I_K) &:= \alpha\left(x\sqrt{(1+g)\eta_- K}-\frac{x}{2}\right) - \alpha\left(x\sqrt{\eta_- K}-\frac{x}{2}\right) \\ &\quad + x\sqrt{\eta_- K}\beta\left(x\sqrt{\eta_- K}-\frac{x}{2}\right) - x\sqrt{(1+g)\eta_- K}\beta\left(x\sqrt{(1+g)\eta_- K}-\frac{x}{2}\right), \end{aligned} \tag{B.7}$$

and

$$\begin{aligned} f_1^+(\xi, I_K) &:= \alpha\left(\frac{2}{x}-1+\left(1+\frac{x}{2}\right)\sqrt{\frac{\omega}{2}}\right) - \alpha\left((2-x)\sqrt{\eta_0 K}+\left(1+\frac{x}{2}\right)\sqrt{\frac{\omega}{2}}\right) \\ &\quad + 2\sqrt{\eta_0 K}\beta\left((2-x)\sqrt{\eta_0 K}+\left(1+\frac{x}{2}\right)\sqrt{\frac{\omega}{2}}\right) - \frac{2}{x}\beta\left(\frac{2}{x}-1+\left(1+\frac{x}{2}\right)\sqrt{\frac{\omega}{2}}\right), \\ f_2^+(\xi, I_K) &:= \alpha\left((2-x)\sqrt{(1+g)\eta_0 K}+\left(1+\frac{x}{2}\right)\sqrt{\frac{\omega}{2}}\right) - \alpha\left((2-x)\sqrt{\eta_0 K}+\left(1+\frac{x}{2}\right)\sqrt{\frac{\omega}{2}}\right) \end{aligned}$$

$$+2\sqrt{\eta_0 K}\beta\left((2-x)\sqrt{\eta_0 K}+\left(1+\frac{x}{2}\right)\sqrt{\frac{\omega}{2}}\right)$$
$$-2\sqrt{(1+g)\eta_0 K}\beta\left((2-x)\sqrt{(1+g)\eta_0 K}+\left(1+\frac{x}{2}\right)\sqrt{\frac{\omega}{2}}\right). \tag{B.8}$$

Similarly,

$$\sum_{N\in\mathbb{Z}_*} Q_{N,0}(\xi, I_K) \sim \frac{1}{\pi\eta_- gK}\frac{1}{(1-x)(2-x)^2}$$
$$\times\begin{cases}0 & \text{for} \quad \sqrt{\dfrac{\eta_-}{(1+g)K}} \geqslant \xi \\ g_1^-(\xi, I_K) & \text{for} \quad \sqrt{\dfrac{1}{(1+g)\eta_- K}} < \xi \leqslant \sqrt{\dfrac{1}{\eta_- K}} \\ g_2^-(\xi, I_K) & \text{for} \quad \sqrt{\dfrac{1}{\eta_- K}} < \xi\end{cases}$$
$$+\frac{\omega}{2\pi\eta_0 gK}\frac{1}{(1-x)x^2}\begin{cases}0 & \text{for} \quad \sqrt{\dfrac{\omega}{2(1+g)\eta_0 K}} \geqslant \xi \\ g_1^+(\xi, I_K) & \text{for} \quad \sqrt{\dfrac{\omega}{2\eta_0(1+g)K}} < \xi \leqslant \sqrt{\dfrac{\omega}{2\eta_0 K}} \\ g_2^+(\xi, I_K) & \text{for} \quad \sqrt{\dfrac{\omega}{2\eta_0 K}} < \xi,\end{cases} \tag{B.9}$$

where

$$g_1^-(\xi, I_K) := \alpha\left(\frac{2}{x}-1+\frac{x}{2}\right)-\alpha\left((2-x)\sqrt{\eta_- K}+\frac{x}{2}\right)$$
$$+2\sqrt{\eta_- K}\beta\left((2-x)\sqrt{\eta_- K}+\frac{x}{2}\right)-\frac{2}{x}\beta\left(\frac{2}{x}-1+\frac{x}{2}\right),$$
$$g_2^-(\xi, I_K) := \alpha\left(\frac{x}{2}+(2-x)\sqrt{(1+g)\eta_- K}\right)-\alpha\left(\frac{x}{2}+(2-x)\sqrt{\eta_- K}\right)$$
$$+2\sqrt{\eta_- K}\beta\left((2-x)\sqrt{\eta_- K}+\frac{x}{2}\right)-2\sqrt{(1+g)\eta_- K}\beta\left((2-x)\sqrt{(1+g)\eta_- K}+\frac{x}{2}\right), \tag{B.10}$$

and

$$g_1^+(\xi, I_K) := \alpha\left(\sqrt{\frac{2}{\omega}}-1-\frac{x}{2}\right)-\alpha\left(x\sqrt{\frac{2\eta_0}{\omega}K}-\left(1+\frac{x}{2}\right)\right)$$
$$+x\sqrt{\frac{2\eta_0}{\omega}K}\beta\left(x\sqrt{\frac{2\eta_0}{\omega}K}-\left(1+\frac{x}{2}\right)\right)-\sqrt{\frac{2}{\omega}}\beta\left(\sqrt{\frac{2}{\omega}}-\left(1+\frac{x}{2}\right)\right),$$
$$g_2^+(\xi, I_K) := \alpha\left(x\sqrt{(1+g)\frac{2\eta_0}{\omega}K}-\left(1+\frac{x}{2}\right)\right)-\alpha\left(x\sqrt{\frac{2\eta_0}{\omega}K}-\left(1+\frac{x}{2}\right)\right)$$
$$+\sqrt{\frac{2\eta_0}{\omega}K}x\beta\left(x\sqrt{\frac{2\eta_0}{\omega}K}-\left(1+\frac{x}{2}\right)\right)-\sqrt{(1+g)\frac{2\eta_0}{\omega}K}x\beta\left(x\sqrt{(1+g)\frac{2\eta_0}{\omega}K}-\left(1+\frac{x}{2}\right)\right). \tag{B.11}$$

Above, we have made use of the periodic functions α and β, which we define via their Fourier series,

$$\alpha(t) := \frac{1}{\pi} \sum_{n \in \mathbb{Z}_*} \frac{e^{\pi i n t}}{n^2} = \frac{2}{\pi} \sum_{n \in \mathbb{N}} \frac{\cos \pi n t}{n^2} \tag{B.12}$$

and

$$\beta(t) := i \sum_{n \in \mathbb{Z}_*} \frac{e^{\pi i n t}}{n} = -2 \sum_{n \in \mathbb{N}} \frac{\sin \pi n t}{n}. \tag{B.13}$$

References

[1] Courant R 1923 *Nach. Ges. Wiss. Göttingen Math.—Phys. Kl.* 81–4
[2] Blum G, Gnutzmann S and Smilansky U 2002 *Phys. Rev. Lett.* **88** 114101
[3] Smilansky U and Sankaranarayanan R 2005 *Proc. Natl Conf. on Nonlinear Systems and Dynamics* (India: Aligarh Muslim University) p 195
[4] Havas P 1975 *J. Math. Phys.* **16** 1461
[5] Berry M V 1977 *J. Phys. A: Math. Gen.* **10** 2083
[6] Bogomolny E and Schmit C 2002 *Phys. Rev. Lett.* **88** 114102
[7] Keating J P, Marklof J and Williams I G 2006 *Phys. Rev. Lett.* **97** 034101
[8] Gnutzmann S, Karageoge P and Smilansky U 2006 *Phys. Rev. Lett.* **97** 090201
[9] Gnutzmann S, Smilansky U and Sondergaard N 2005 *J. Phys. A: Math. Gen.* **38** 8921–33
[10] Brüning J, Klawonn D and Puhle C 2007 Remarks on 'Resolving isospectral 'drums' by counting nodal domains' *J. Phys. A: Math. Theor.* **40** 15143–7
[11] Band R, Oren I and Smilansky U 2008 Nodal domains on graphs—how to count them and why? *Preprint* 0711.3416v2
[12] Kac M 1966 *Am. Math. Mon.* **73** 1–23
[13] Zelditch S 1998 *J. Diff. Geom.* **49** 207
[14] Bleher P M 1994 *Duke Math. J.* **74** 45–93
[15] Gurarie D 1995 *J. Math. Phys.* **36** 4
[16] Marklof J 1998 *Commun. Math. Phys.* **199** 169–202
[17] C de Verdière Y 1980 *Math. Z.* **171** 51–73
[18] Bleher P M, Kosygin D V and Sinai Y 1995 *Commun. Math. Phys.* **170** 375–403
[19] Besse A L 1978 *Manifolds all of Whose Geodesics are Closed* (Berlin: Springer)
[20] Aronovitch A 2008 private communication